

3,5,7-Substituted Pyrazolo[4,3-*d*]pyrimidine Inhibitors of Cyclin-Dependent Kinases and Their Evaluation in Lymphoma Models

Radek Jorda,[†] Libor Havlíček,[‡] Antonín Šturm,[‡] Diana Tušková,[§] Lenka Daumová,[§] Mahmudul Alam,[§] Jana Škerlová,^{||,⊥} Michaela Nekardová,^{||,⊥} Miroslav Peřina,[†] Tomáš Pospíšil,[†] Jitka Šíroková,[†] Lubor Urbánek,[†] Petr Páchl,^{||} Pavlína Řezáčová,^{||,⊥} Miroslav Strnad,[†] Pavel Klener,[§] and Vladimír Kryštof^{*,†}

[†]Laboratory of Growth Regulators, Palacký University and Institute of Experimental Botany, The Czech Academy of Sciences, Šlechtitelů 27, 783 71 Olomouc, Czech Republic

[‡]Isotope Laboratory, Institute of Experimental Botany, The Czech Academy of Sciences, Vídeňská 1083, 142 20 Prague, Czech Republic

[§]Institute of Pathological Physiology, First Faculty of Medicine, Charles University, 128 53 Prague, Czech Republic

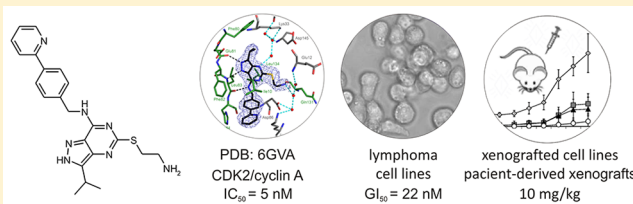
^{||}Institute of Organic Chemistry and Biochemistry, The Czech Academy of Sciences, Flemingovo nám. 2, 166 10 Prague 6, Czech Republic

[⊥]Institute of Molecular Genetics, The Czech Academy of Sciences, Vídeňská 1083, 142 20 Prague, Czech Republic

[#]Faculty of Mathematics and Physics, Charles University in Prague, Ke Karlovu 3, 121 16 Prague 2, Czech Republic

S Supporting Information

ABSTRACT: Cyclin-dependent kinases are therapeutic targets frequently deregulated in various cancers. By convenient alkylation of the 5-sulfanyl group, we synthesized 3-isopropyl-7-[4-(2-pyridyl)benzyl]amino-1(2)*H*-pyrazolo[4,3-*d*]pyrimidines with various substitutions at position 5 with potent antiproliferative activity in non-Hodgkin lymphoma cell lines. The most potent derivative **4.35** also displayed activities across more than 60 cancer cell lines. The kinase profiling confirmed high selectivity of **4.35** toward cyclin-dependent kinases (CDKs) 2, 5, and 9, and the cocrystal with CDK2/cyclin A2 revealed its binding in the active site. Cultured lymphoma cell lines treated with **4.35** showed dephosphorylation of CDK substrates, cleavage of PARP-1, downregulation of XIAP and MCL-1, and activation of caspases, which collectively confirmed ongoing apoptosis. Moreover, **4.35** demonstrated significant activity in various cell line xenograft and patient-derived xenograft mouse models *in vivo* both as a monotherapy and as a combination therapy with the BCL2-targeting venetoclax. These findings support further studies of combinatorial treatment based on CDK inhibitors.



INTRODUCTION

Non-Hodgkin lymphomas (NHLs) are the most frequent hematologic malignancies in the western hemisphere, comprising approximately 30% of all hematologic cancers. Based on the behavior of the cancer, NHLs can be classified as indolent, aggressive, and highly aggressive lymphomas. The latter two NHL types include diffuse large B-cell lymphoma, Burkitt's lymphoma, mantle cell lymphoma, and peripheral T-cell lymphomas. The deregulation of cell cycle machinery and the disruption of programmed cell death are hallmarks of aggressive NHL. These hallmarks include mutated or overexpressed oncogenes (e.g., MYC, BCL6, MYD88, cyclin D1, BCL2, and CDK4/6) or the deletion of tumor suppressors (e.g., TP53, TP63, RB1, CDKN2A, and ATM). Double- and triple-hit lymphomas characterized by the concurrent genetic aberrations of MYC, BCL-2, and/or BCL6 represent a subgroup of NHL with an extremely dismal prognosis.¹

Some of the recurrently overexpressed or mutated genes encode drug targets, such as BCL-2 protein, Bruton's tyrosine kinase or phosphoinositide 3-kinase, which can be modulated by the small-molecule inhibitors venetoclax, ibrutinib or idelalisib, respectively.^{2–4} Another emerging pharmacological approach targets cyclin-dependent kinases (CDKs), which were first discovered for their role in regulating the cell cycle.⁵ Depending on their selectivity, CDK inhibitors can interfere either with cell cycle progression by blocking RB protein phosphorylation (governed by CDKs 2/4/6) or with global transcription by inactivating RNA polymerase II (governed by CDKs 7/8/9/12). However, many inhibitors have broad specificity and simultaneously obstruct both of these processes,^{6–8} providing the advantage of overcoming possible compensatory functions among the CDK family.⁹

Received: January 30, 2019

Published: April 3, 2019

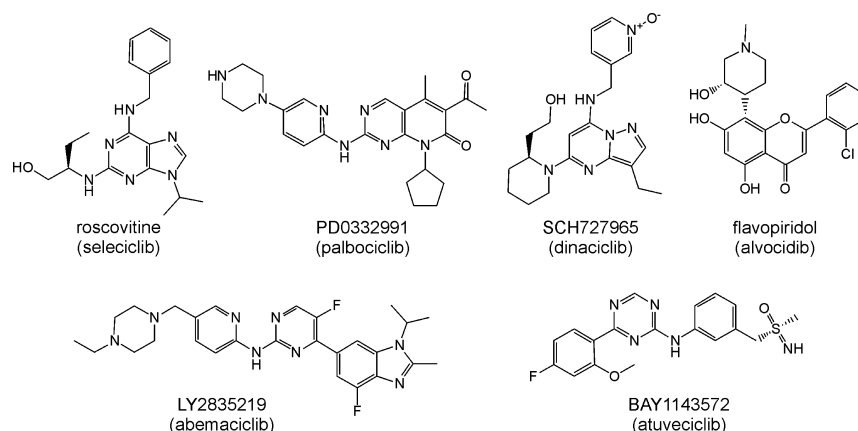
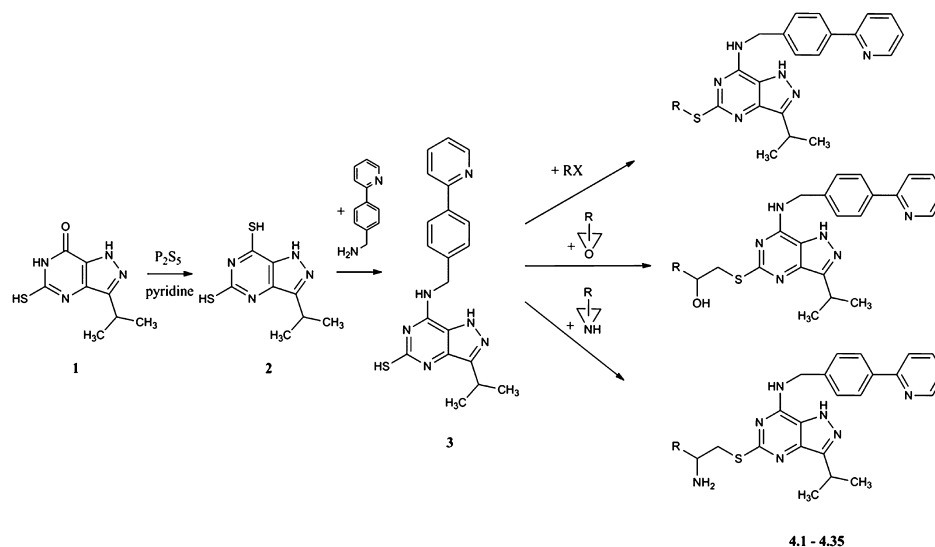


Figure 1. Some cyclin-dependent kinase inhibitors with activity in lymphomas.

Scheme 1. General Procedure for the Synthesis of Novel 5-Alkylthio-3-isopropyl-7-[4-(2-pyridyl)benzyl]amino-1(2)*H*-pyrazolo[4,3-*d*]pyrimidines



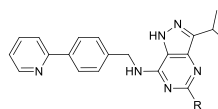
CDK inhibitors, including clinical candidate drugs such as flavopiridol, roscovitine, dinaciclib, and the recently approved drugs palbociclib and abemaciclib, have been increasingly evaluated in various lymphomas (Figure 1).^{10–14} In NHL, similar to other cancers, the pharmacological inhibition of transcriptional CDKs leads to the downregulation of short-lived mRNAs related to cell survival, such as those of MCL-1, XIAP, MYC, and cyclin D1. The downregulation of cyclin D1 and MCL-1 protein levels was observed in mantle cell lymphomas and in aggressive MYC-driven B-cell lymphoma treated with roscovitine and dinaciclib, respectively.^{11,12} Despite the fact that these compounds inhibit multiple CDKs, a widely accepted mechanism of action involves CDK9, which was independently supported by findings obtained with the highly CDK9-selective drug atuveciclib.¹⁵ Importantly, the loss of MCL-1 as a consequence of CDK9 or CDK7 inhibition by these drugs has been found to strongly enhance apoptosis induction in NHL by small-molecule antagonists of BCL-2.^{16–21}

The pan-selective purine CDK inhibitor roscovitine, which was discovered in our laboratory, was among the first CDK inhibitors that entered clinical trials.^{22,23} The further exploration of roscovitine has been mainly oriented toward either modifications in its substitutable positions^{24–26} or the

redistribution of nitrogen atoms of the purine scaffold; the latter approach culminated in nanomolar inhibitors based on pyrazolo[4,3-*d*]pyrimidines and pyrazolo[1,5-*a*][1,3,5]-triazine.^{27–30}

The objective of this work was to synthesize novel potent pyrazolo[4,3-*d*]pyrimidine CDK inhibitors, which proved to be more potent than related purines,^{28–30} and explore their activity toward lymphoma models. The heterocyclic core was substituted with groups that conferred high activity in purines, identified during our previous structure–activity studies;^{24,26} that is, isopropyl moiety at position 3, benzylamines at position 7 and alkyl- or cycloalkyl-amines at position 5.^{29,30} The compounds were prepared using more convenient alkylation of 5-sulfanyl derivatives, providing substantially higher yields over the 5-amino-substituted pyrazolo[4,3-*d*]pyrimidines described earlier.^{30,31} In line with our expectations, the newly prepared derivatives displayed nanomolar potency against CDKs and cancer cell lines. Our previous study demonstrated that roscovitine strongly sensitizes leukemia and lymphoma cells to TRAIL-induced apoptosis by altering the levels of BCL-2 proteins in the mitochondria³² and, together with other observations,¹¹ this led us to explore anticancer activity of new pyrazolo[4,3-*d*]pyrimidines against several lymphoma models. The compounds proved to potently kill various lymphoma cell

Table 1. CDK2/E Inhibitory and Cellular Activities of Novel Pyrazolo[4,3-d]pyrimidines



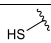
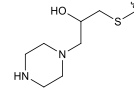
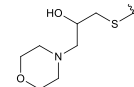
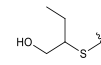
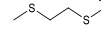
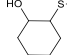
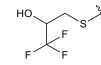
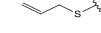

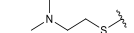
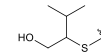
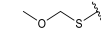
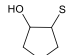
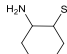
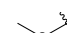
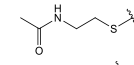
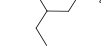
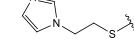
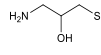

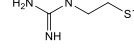
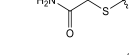
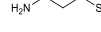
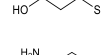
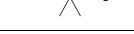
Compound	R - substitution	IC ₅₀ (μM) ^a	GI ₅₀ (μM) ^a	CDK2/E	HT	OCI-LY2	MINO
3		0.558	2.760	3.240	2.175		
4.1		0.171	0.332	0.435	0.767		
4.2		0.156	0.200	0.200	0.243		
4.3		0.15	0.255	0.181	0.119		
4.4		0.138	0.975	0.668	0.773		
4.5		0.134	0.636	0.680	0.530		
4.6		0.132	0.690	0.585	0.641		
4.7		0.100	1.005	0.858	0.923		
4.8		0.099	0.105	0.109	0.076		
4.9		0.077	0.054	0.061	0.093		
4.10		0.077	0.980	1.001	1.307		
4.11		0.059	0.340	0.285	0.243		
4.12		0.052	0.567	0.373	0.450		
4.13		0.052	0.139	0.136	0.157		
4.14		0.048	0.783	1.207	1.050		
4.15		0.041	0.071	0.054	0.042		
4.16		0.039	0.273	0.280	0.427		
4.17		0.032	0.155	0.145	0.135		
4.18		0.031	0.055	0.055	0.064		
4.19		0.030	0.507	0.610	0.477		
4.20		0.030	0.39	0.812	0.39		
4.21		0.027	0.192	0.163	0.197		
4.22		0.022	0.120	0.151	0.156		
4.23		0.021	0.109	0.102	0.089		
4.24		0.020	0.085	0.100	0.064		

Table 1. continued

Compound	R - substitution	CDK2/E	HT	OCI-LY2	MINO
4.25		0.019	0.080	0.053	0.069
4.26		0.019	0.120	0.084	0.081
4.27		0.018	0.240	0.198	0.136
4.28		0.013	0.056	0.092	0.040
4.29		0.012	0.062	0.152	0.081
4.30		0.012	0.480	0.780	0.770
4.31		0.011	0.063	0.099	0.051
4.32		0.010	0.021	0.022	0.010
4.33		0.003	0.048	0.050	0.040
4.34		0.003	0.190	0.141	0.160
4.35		0.002	0.022	0.028	0.041
CR8		0.062	0.263	0.307	0.202
dinaciclib		0.002	0.019	0.011	0.019
ibrutinib		>25	15.9	18.9	10.7

^aMeasured at least in triplicate.

lines and also displayed significant *in vivo* activity both in monotherapy and in a combination with venetoclax, which corresponds to the abovementioned findings.

RESULTS AND DISCUSSION

Design and Synthesis. We recently described 5-alkylamino-3-isopropyl-7-[4-(2-pyridyl)benzyl]amino-1(2)*H*-pyrazolo[4,3-*d*]pyrimidines that share some of the same substitutions as the purine CDK inhibitor roscovitine, but that showed substantially higher potency against CDKs and cancer cell lines than did roscovitine.^{28,30} Because of the laborious synthesis of these derivatives, we sought to improve the synthetic accessibility of these compounds while retaining or even improving their biochemical potency. We focused on the substituted position 5 on the pyrazolo[4,3-*d*]pyrimidine scaffold and report here a new series of 3,5,7-trisubstituted pyrazolo[4,3-*d*]pyrimidines in which the alkylamino group at the 5-position of the heterocycle is replaced by a 5-alkylthio group. To verify the effect of this modification, we employed molecular modeling. We applied the computational procedure delineated in our previous work, in which we identified the pyrazolo[4,3-*d*]pyrimidine core as the most favorable central heterocycle of the purine bioisosteres of CDK2 inhibitors.³³ Importantly, we have shown that the contributions of the central heterocyclic cores and the individual substituents, quantified and evaluated in relation to conformations of the optimized protein-inhibitor complexes, are not simply additive. Depending on the scaffold, the same substituents can be associated with different interaction “free” energies $\Delta G'_{\text{int}}$ (in kcal mol⁻¹). Our preliminary calculations suggested that the replacement of the alkylamino group at the 5-position with the

5-alkylthio group can increase the binding affinity to CDK2 (selected data are available in [Supporting Information](#)).

The new compounds have been prepared from 3-isopropyl-5-sulfanyl-1(2)*H*-pyrazolo[4,3-*d*]pyrimidin-7-ol **1** (synthesized according to a described procedure²⁸), which was first converted to 5,7-dithiol **2** and subsequently substituted at the heterocycle position 7 with 4-(2-pyridyl)benzylamine. The final compounds **4** were prepared by the alkylation of the reactive 5-sulfanyl functional group of **3** by various agents ([Scheme 1](#)); in the final step, we successfully prepared 24 alkyl halogens (yielding compounds **4.2–4.4**, **4.6–4.11**, **4.17**, **4.18**, **4.21–4.23**, **4.25**, **4.26**, **4.28**, **4.30–4.33**, and **4.35**), 8 epoxides (yielding compounds **4.1**, **4.5**, **4.12**, **4.16**, **4.19**, **4.29**, **4.33**, and **4.34**), and aziridines (yielding compounds **4.13**, **4.24**, and **4.35**).

The reactivity of the sulfanyl functional group enables the use of different classes of alkylating agents, eventually leading to the same compounds with similar yields (**4.33** and **4.35** were prepared not only by using alkyl halogens but also by using suitable epoxide or aziridine, respectively). This new synthetic approach overcomes the less convenient nucleophilic aromatic substitution ($S_{\text{N}}\text{Ar}$, which requires difficult reaction conditions, makes undesired byreactions and subsequently byproducts) described in our previous article examining 5-alkylamino-1(2)*H*-pyrazolo[4,3-*d*]pyrimidine derivatives.³⁰

Structure–Activity Relationships. The implementation of the most suitable substitution at the 5 position of the pyrazolo[4,3-*d*]pyrimidine core was mostly inspired by previous structure–activity relationship studies on trisubstituted pyrazolo[4,3-*d*]pyrimidine CDK inhibitors,^{29,30} related purines,^{26,34–37} and pyrazolo[1,5-*a*]pyrimidines.³⁸ The compounds we prepared included inhibitors with significant

activity against CDK2/E; all compounds exhibited an IC_{50} below 200 nM, and approximately 50% of inhibitors blocked the activity of the simple 5-methylthio derivative **4.14** (IC_{50} = 48 nM). The substituent in position 5 is mostly in contact with the flexible parts of the enzyme surface or with the solvent (water molecules) and therefore can be more variable, whereas the side chains at positions 3 and 7 do not allow such variability. Despite low differences in the CDK2 inhibition measured with the studied compounds, we found some relationships that are associated with the size/length of the substituent at position 5 or its polarity. Compound **3**, which contains an acidic sulfanyl functional group in position 5, was the weakest in the series, with nearly three-fold lower potency than an analogous 3,7-disubstituted compound described earlier.³⁰ The methylation of the 5-sulfanyl functional group results in short lipophilic substituents in **4.14**, increasing the potency more than ten-fold.

The weakest CDK2 inhibition (IC_{50} between 100–200 nM) was observed for compounds bearing rigid piperazine and morpholine moieties (**4.2** and **4.1**, respectively). Additional groups with weak activity against CDK2 included compounds with less polar (**4.4**, **4.7**, **4.11**, and **4.14**) or cycloalkyl (**4.5**, **4.12**, and **4.13**) substituents at position 5 or those with tertiary amino groups (**4.8** and **4.9**) (IC_{50} = 48–138 nM). In contrast, the most potent inhibitors of the series (IC_{50} = 2–39 nM) bear at least one polar group (mainly a hydroxy or primary amino group) placed either on a short linear (**4.35**, **4.33**, **4.22**, **4.23**, and **4.28**) or on a small branched chain (**4.34**, **4.32**, **4.30**, **4.29**, **4.27**, and **4.26**). Further modification of 2-aminoethylthio in the most active compound **4.35** led to the impairment of CDK2 inhibition; this effect was observed when the terminal amino group was modified by methylation, acetylation, and conversion to urea or guanidine (**4.28**, **4.15**, **4.9**, **4.27**, and **4.20**, respectively) and is probably due to steric hindrance due to possible hydrogen bonding, increased basicity of the amine (**4.28** and **4.20**), or a combination of both. Other attempts to modify the primary amine in **4.35** diminished its activity, such as its extension with aminomethyl (**4.30**) or its cyclization (**4.13** and **4.17**). A similar scenario is also evident for the modified hydroxyethylthio derivatives, among which only compound **4.34** reached the same potency as the analog **4.33**; all other compounds (**4.32**, **4.29**, **4.19**, **4.18**, **4.16**, **4.12**, **4.11**, **4.5**, **4.3**, **4.2**, **4.1**, and **4.31**) have worse CDK2 inhibition.

Recent experiments have shown that pharmacological CDK inhibition is an effective and rational treatment option for aggressive MYC-driven lymphomas.¹¹ We therefore screened all prepared compounds against the non-NHL cell lines HT, OCI-LY2, and MINO.

The antiproliferative activity of the prepared compounds was consistent with enhanced CDK2 inhibition (Table 1). The most potent compounds, **4.28**, **4.29**, **4.31**, **4.32**, **4.33**, **4.34**, and **4.35** had notably improved potency compared with the related purine CR8, with an average GI_{50} value fivefold higher than that of CR8.

Crystal Structure of the Complex of CDK2/Cyclin A2 with Pyrazolo[4,3-*d*]pyrimidine 4.35. To obtain structural insights into the interaction of our inhibitors with the enzyme, we determined the crystal structure of the active Thr160-phosphorylated CDK2 with a fragment of cyclin A2 (residues 175–432) in complex with compound **4.35** at 2.15 Å resolution (PDB code: 6GVA). For data collection and refinement statistics, see Table S2. The asymmetric unit contains one CDK2/cyclin A2 heterodimer. The residues 39–

40 and C-terminal residues 291–298 of CDK2 could not be modeled into the electron density map because of disorder.

The inhibitor binds to the active site located in a narrow cleft between the N- and C-terminal domains of CDK2 in the standard binding mode typical for pyrazolo[4,3-*d*]pyrimidine-based inhibitors (see Figure 2). Specifically, the pyrazolo[4,3-

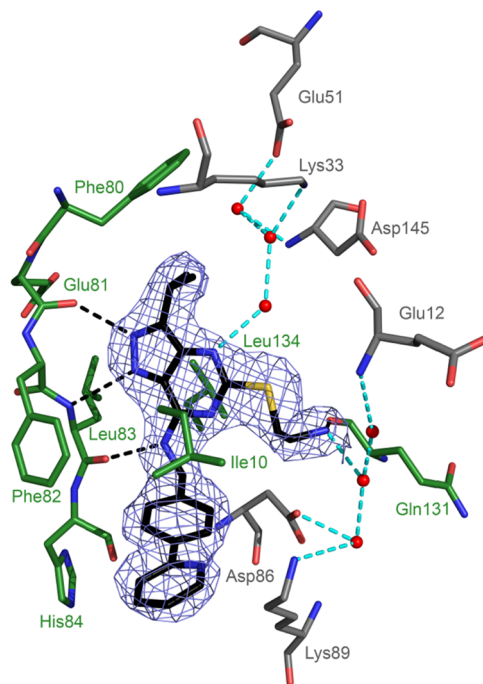


Figure 2. Inhibitor **4.35** bound to the active site of CDK2 (PDB: 6GVA). CDK2 residues interacting with the inhibitor directly (black dashed lines) or through water molecules (cyan dashed lines and red spheres) are shown in green or gray stick representations, respectively. A refined $2F_o - F_c$ electron density map for the inhibitor contoured at 1σ is shown.

d]pyrimidine core is sandwiched between the hydrophobic side chains of Ile10 and Leu134 and interacts via three conserved hydrogen bonds with the hinge region residues (7-amino N–H···O:Leu83, N2–H···O:Glu81, and a weak N1···HN:Leu83 bond). The R³ isopropyl group forms hydrophobic interactions with the gatekeeper residue Phe80. The terminal amino group of the R⁵ moiety forms a hydrogen bond with the carbonyl oxygen of Gln131 from the phosphate-ribose pocket. The proximal phenyl ring of the R⁷ moiety is sandwiched between Ile10 and the backbone of His84, close to the specificity surface. The terminal pyridine ring sticks out of the binding cleft, roughly in plane with the proximal phenyl ring. Moreover, N4 from the pyrazolo[4,3-*d*]pyrimidine core of the inhibitor interacts through a chain of three water molecules (W414, W435, and W436) with the side chains of Lys33 and Glu51 and with the main chain of Asp145. Another chain of three water molecules (W409, W426, and W471) provides additional hydrogen bonding of the amino group on the R⁵ moiety to the main chain of Glu12 and to the side chains of Asp86 and Lys89 at the edge of the binding cleft.

Kinase Selectivity. As the most potent compound, **4.35** was then assayed on a panel of related CDKs. **4.35** had low nanomolar activity not only against CDK2 but also against CDK5 and CDK9 (Table 2). The compound displayed at least 10-fold increased potency toward most of the assayed CDKs

Table 2. CDK Selectivity Profile of Pyrazolo[4,3-*d*]pyrimidine 4.35 (CR8 and Dinaciclib Assayed as Controls)

kinase	IC ₅₀ (μM) ^a		
	4.35	CR8	dinaciclib
CDK1/B1	0.090 ± 0.012	0.787 ± 0.100	0.072 ± 0.024
CDK2/E1	0.002 ± 0.001	0.062 ± 0.026	0.002 ± 0.001
CDK2/A2	0.006 ± 0.003	0.144 ± 0.002	0.003 ± 0.001
CDK4/D1	0.603 ± 0.318	26.09	0.115 ± 0.018
CDK5/p25	0.015 ± 0.003	0.225 ± 0.013	0.067 ± 0.032
CDK7/H/MAT	0.124 ± 0.007	1.769 ± 0.013	0.170 ± 0.008
CDK9/T1	0.025 ± 0.002	0.272 ± 0.038	0.015 ± 0.006

^aMeasured at least in triplicate.

compared to the related purine CR8, with the highest increase (43-fold) toward CDK4/cyclin D1.

Next, preliminary selectivity profiling of 4.35 was performed on a panel of 50 additional protein kinases, a representative sampling of the human kinome. The compound was assayed at a single concentration of 1 μM. As shown in Table S3, significant inhibition was observed for CK1δ and CHK2; the residual activity of these kinases decreased to 11 and 18%, respectively. We then determined the IC₅₀ values for CK1δ and CHK2 (0.045 and 0.525 μM, respectively). Weak inhibition of PAK4, CAMK1, or RSK1 kinases was also observed; these kinases are known to be sensitive to related CDK inhibitors with pyrazolo[4,3-*d*]pyrimidine or purine scaffolds.^{29,39–41} These results confirmed the reasonable selectivity of 4.35.

Antiproliferative Effects. We next assessed the anticancer activity of 4.35 against additional lymphoma cell lines as well as other human cancer cell lines (Table 3). 4.35 displayed a broad range of activity across all assayed cell lines, with the average concentration to reduce cell proliferation by 50% (GI₅₀ value) of 21.6 nM. The most sensitive cell lines were the diffuse large B-cell lymphomas OCI-LY3, RIVA, and HBL-1. The clinical candidate dinaciclib, assayed in parallel, displayed similar potency.

To further assess the anticancer selectivity of 4.35, we also screened the NCI60 cell line panel. Notably, 4.35 robustly inhibited proliferation across the entire cancer cell line panel with a mean GI₅₀ of 23 nM (Table S4). In general, 4.35 was effective against leukemia, melanoma, and breast cancer cells but showed decreased activity in ovarian and renal cells.

Mechanism of Action in Cells. Compound 4.35 emerged as the most potent CDK inhibitor in this series, and because of its superior proapoptotic activity in several lymphoma cell lines (Figures S6 and S7), we sought to characterize its cellular effects. We therefore performed immunoblotting analyses of MINO cells exposed to 4.35 both at different doses and for different lengths of time. The treated cells contained clear markers of ongoing apoptotic cell death, including the appearance of the PARP-1 fragment (89 kDa), diminution of full-length PARP-1, activation of caspases 3 and 7, and reduction in the levels of the anti-apoptotic proteins MCL-1 and XIAP (Figure 3A,B). On the other hand, the anti-apoptotic proteins BCL-2 and BCL-XL did not show any change, probably because of their high stability. Clear markers of apoptosis were also detected in UPF1H and MAVER-1 cells (Figure S8). These results are consistent with the known mechanisms of the pro-apoptotic action of other CDK inhibitors.^{11,12,24,30}

Table 3. Effect of Pyrazolo[4,3-*d*]pyrimidine 4.35 on Various Human Cancer Cell Lines

cancer type	cell line	IC ₅₀ (μM) ^a	
		4.35	dinaciclib
lymphoma (DLBCL-ABC)	RIVA	0.011	0.031
	OCI-LY3	0.007	n.d.
	U2932	0.030	0.011
	HBL-1	0.010	0.013
	TMD8	0.012	0.017
lymphoma (DLBCL-GCB)	OCI-LY2	0.023	0.011
	OCI-LY7	0.014	0.002
	SU-DHL10	0.017	n.d.
	SU-DHL4	0.015	0.010
	HT	0.019	0.019
lymphoma (MCL)	HBL-2	0.043	0.013
	JEKO-1	0.014	0.014
	MAVER-1	0.013	0.017
	MINO	0.016	0.011
	UPF1H	0.025	0.013
lymphoma (BL)	UPF7U	0.012	0.019
	Z138	0.013	n.d.
	Ramos	0.044	0.015
leukemia (CML)	Raji	0.038	0.025
	K562	0.036	0.011
leukemia (ALL)	CEM	0.033	0.007
leukemia (AML)	THP-1	0.019	0.007
multiple myeloma	RPMI8226	0.015	0.009
Breast	MCF-7	0.016	0.006
Cervix	HeLa	0.017	0.013
Colon	HCT-116	0.022	0.007
Melanoma	G361	0.036	0.016

^aMeasured at least in triplicate; DLBCL-ABC, diffuse large B-cell lymphoma, subtype-activated B-cell; DLBCL-GCB, diffuse large B-cell lymphoma, subtype-germinal center B-cell; MCL—mantle cell lymphoma; BL—Burkitt lymphoma; CML, chronic myelogenous leukemia; ALL, acute lymphoblastic leukemia; AML, acute monocytic leukemia.

The kinetics of CDK inhibition by 4.35 was studied in MINO cells over the period of 24 h (Figure 3C). The dose of 12.5 nM was selected because it induced a strong response within 24 h in previous experiments (Figure 3A,B), and it was anticipated that CDK inhibition would be evident at earlier time points. Importantly, a gradual decrease in the phosphorylation of the C-terminus of RNA polymerase II (at serines 2 and 5) and retinoblastoma protein (at serines 608 and 780) in a time-dependent manner was observed, suggesting that at least CDK2, CDK7, and CDK9 were effectively inhibited.

In Vivo Activity: Monotherapy. The in vivo efficacy of 4.35 was then assessed in murine models of aggressive lymphomas based on subcutaneous xenotransplantation of three established lymphoma cell lines (MINO, MAVER-1, and HBL-2) and one patient-derived lymphoma xenograft (PDX—VFN-M1) in immunodeficient mice. Because of relatively rapid pharmacokinetics and limited oral availability (for details, see Supporting Information), compound 4.35 was administered daily by intravenous (iv) injections. Treatment with 4.35 was associated with a significant reduction in the growth of all three xenografted lymphoma cell lines compared to controls (Figure 4). Importantly, anti-lymphoma activity was also clearly achieved in the PDX mouse model VFN-M1, which represents

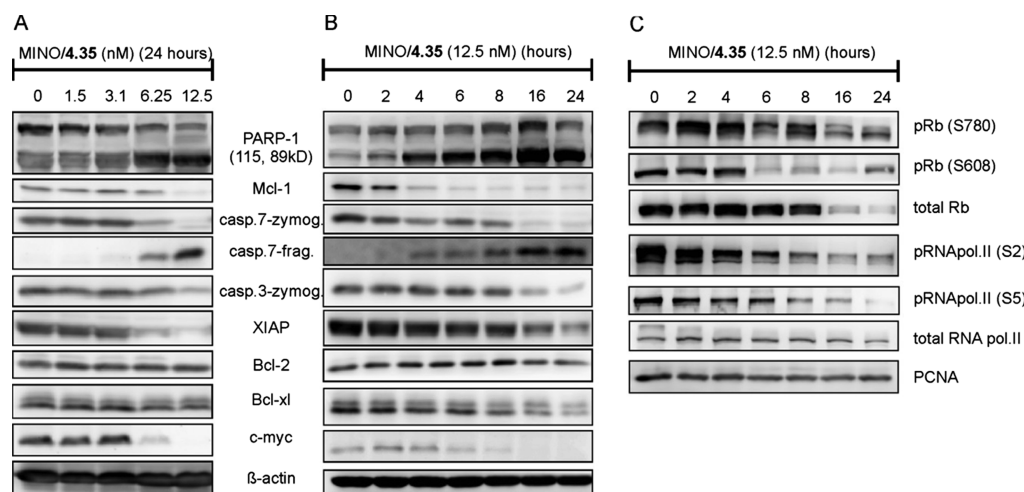


Figure 3. Immunoblotting analysis of expression of CDK substrates and apoptosis-related proteins in MINO lymphoma cells treated with 4.35 in a dose- (A) and time-dependent (B,C) manner.

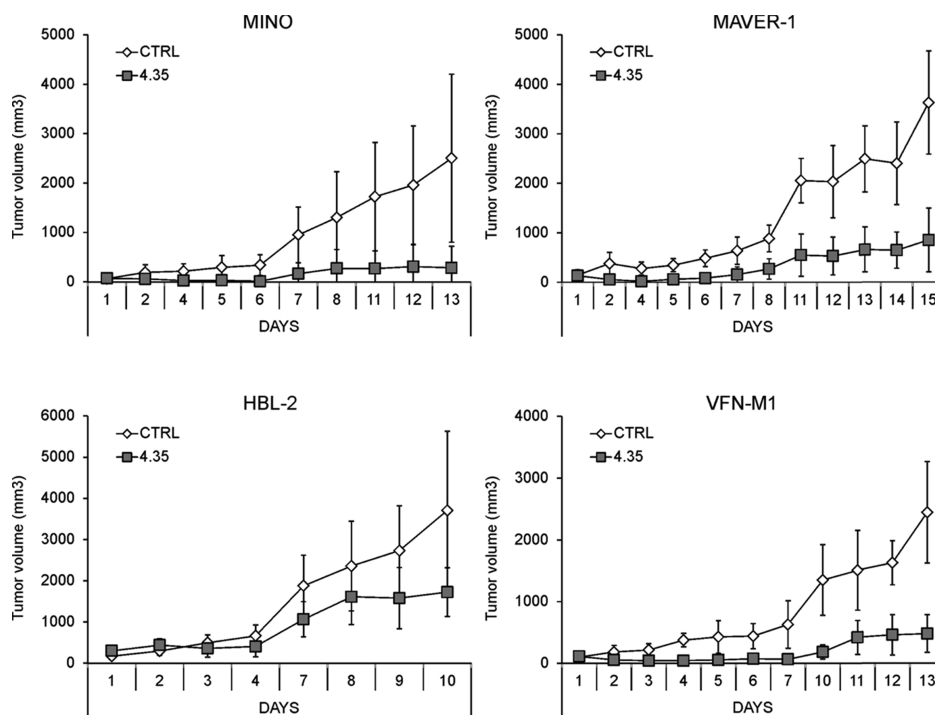


Figure 4. Determination of tumor volume of vehicle- or 4.35-treated (10 mg/kg) mice after iv dosing in MINO ($n = 10$), MAVER-1 ($n = 12$), Hbl-2 ($n = 8$) and VFN-M1 patient-derived xenograft (PDX, $n = 10$).

a surrogate model for primary lymphoma cells from patients (Figure 4).

Ex vivo analysis of selected pharmacodynamic targets of 4.35 in subcutaneously grown lymphoma tumors 24 h after a single iv administration of 4.35 confirmed the induction of apoptosis and the downregulation of MCL-1 and XIAP proteins but had no impact on the expression of BCL-2 (Figures 5 and S10). Notably, the changes were also evident in the PDX model VFN-M1, a reliable surrogate for the primary cells of patients (Figure 5C). In addition, reduced RB and RNA polymerase II phosphorylation at several phosphorylation sites was also observed (Figure S11).

In Vivo Activity: A Combination with Venetoclax. We and others have previously demonstrated that the concurrent inhibition of BCL-2 and MCL-1 results in marked cytotoxic

synergy in lymphoma models.^{42,43} A loss of the antiapoptotic protein MCL-1 observed in the cell line and xenograft lymphoma models treated with 4.35 (Figures 3 and 5) suggests that the depletion may confer the lymphoma cell dependency on other BCL2 family members. Therefore, we investigated the response of a MAVER-1 xenograft to the combination 4.35 and venetoclax (ABT199), an inhibitor of BCL-2 family proteins. The individual treatment of both compounds, 4.35 and venetoclax, significantly inhibited tumor growth. Importantly, the inhibitory effect was more pronounced when the mice were treated with a combination of these compounds, and the tumors did not start to expand over the observed time period (Figure 6). The results are in line with recent observations made with the CDK inhibitor

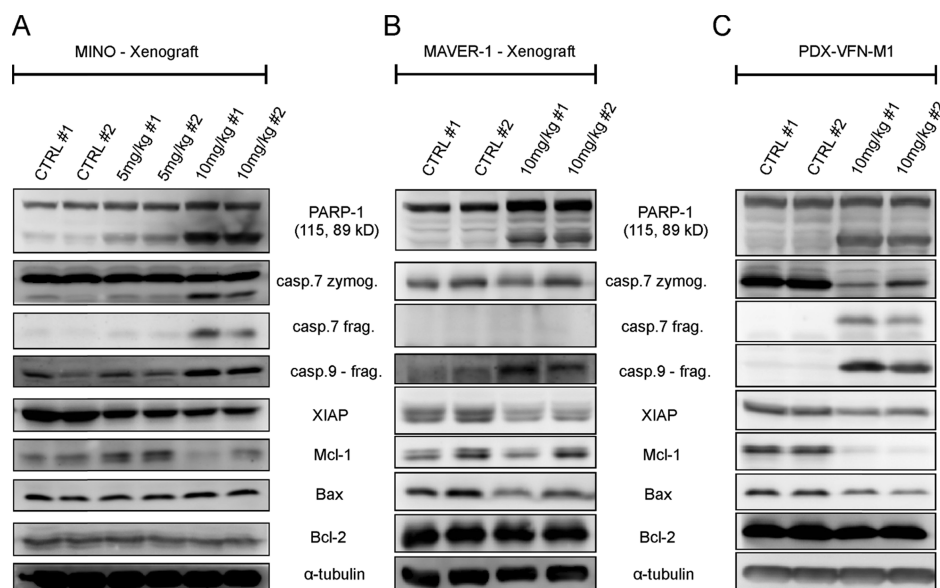


Figure 5. Inhibitory effect of pyrazolo[4,3-*d*]pyrimidine 4.35 on the growth of lymphoma xenografts derived from the MINO (A) and MAVER-1 (B) cell lines and from patient-derived VFN-M1 cells (C). Tumor-bearing mice were intravenously injected with 4.35. After 24 h, the mice were euthanized, and the tumors were removed and investigated for the expression of apoptosis markers. Each lane represents a different animal.

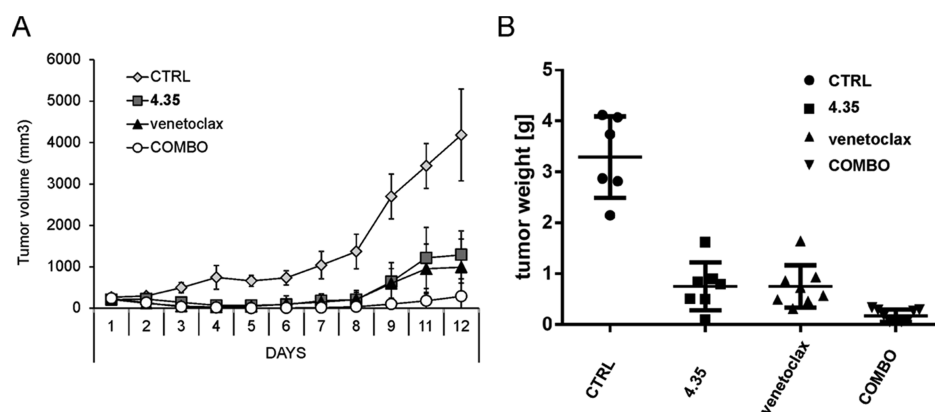


Figure 6. Combination of 4.35 and venetoclax in MAVER-1 xenografts. (A) Mean calculated tumor volumes (\pm SD) of MAVER-1 subcutaneously (sc) tumors from the initiation of therapy (day 1). MAVER-1 cells were xenografted to NSG mice and treated with vehicle (control, $n = 6$), 4.35 (9 mg/kg, $n = 8$), venetoclax (20 mg/kg, $n = 8$), or 4.35 + venetoclax combination ($n = 10$). (B) Evaluation of the mean calculated tumor weight (\pm SD) of MAVER-1 sc tumors from the abovementioned therapies (= day 13).

dinaciclib, which clearly sensitized MYC-BCL-2 double-hit lymphomas to the BCL-2 inhibitor venetoclax.^{17,19}

CONCLUSIONS

Relatively slow progression of pan-CDK inhibitors in clinical trials, which is generally attributed to their complicated mechanisms of action, narrow therapeutic windows, and the lack of robust patient selection criteria collectively emphasize the necessity to develop and explore new compounds with altered kinase profile. Herein, we describe the synthesis and biological activity of new pyrazolo[4,3-*d*]pyrimidines that potentially inhibited cyclin-dependent kinase 2 as demonstrated by biochemical assays and crystallographic analysis. Our findings confirmed the *in vitro* and *in vivo* sensitivity of aggressive non-NHLs to CDK inhibitors and provide rationale for their future clinical evaluation. In addition, the combination of CDK inhibitors selected based on the biological mechanism (targeting predominantly MCL-1) and the BCL-2 targeting agent venetoclax proven to exert synergistic effects exhibit

synthetic lethality *in vivo* and should be considered for combinatorial treatment approaches in patients.

EXPERIMENTAL SECTION

NMR spectra were recorded on a JEOL ECA-500 spectrometer operating at the frequencies of 500.16 MHz (¹H) and 125.76 MHz (¹³C). ¹H NMR and ¹³C NMR chemical shifts were referenced to the solvent signals; for ¹H, δ (residual CHCl₃) = 7.25 ppm, δ (residual DMSO-*d*₅) = 2.50 ppm, δ (residual CD₃OD) = 3.31 ppm; ¹³C: δ (CDCl₃) = 77.23 ppm, δ (DMSO-*d*₆) = 39.52 ppm, and δ (CD₃OD) = 49.15 ppm. Chemical shifts are provided in the δ scale [ppm] and the coupling constants are provided in Hz.

Melting points were determined on a Kofler block and are uncorrected. Reagents were of analytical grade and obtained from standard commercial sources or were synthesized according to the referenced procedure. Thin-layer chromatography was performed using aluminum sheets with silica gel F254 from Merck. Spots were visualized under UV light (254 nm). ESI or APCI mass spectra were determined using a Waters Micromass ZMD mass spectrometer (sample solution in MeOH, direct inlet, coin voltage was in the range of 10–30 V, trace amounts of HCOOH or NH₄OH was used to

influence ionization). Column chromatography was performed using Merck silica gel Kieselgel 60 (230–400 mesh). The purity of all synthesized compounds was determined by high-performance liquid chromatography-photo diode array (200–500 nm) and gave satisfactory results (>95%). Specific optical rotation was measured on a polarimeter polAAR 3001 (wave length: 589.0 nm, tube length: 50 mm, at 23 °C). All compounds gave satisfactory elemental analyses ($\pm 0.4\%$).

3-Isopropyl-5-sulfanyl-1(2)*H*-pyrazolo[4,3-*d*]pyrimidin-7-ol (1). This compound was prepared according to the literature.²⁸

3-Isopropyl-1(2)*H*-pyrazolo[4,3-*d*]pyrimidine-5,7-dithiol (2). 3-Isopropyl-5-sulfanyl-1(2)*H*-pyrazolo[4,3-*d*]pyrimidin-7-ol (1) (74 g, 0.35 mol) was added to a solution of phosphorus pentasulfide (93 g, 0.42 mol) in pyridine (550 mL) at 75 °C. The reaction mixture under nitrogen was refluxed for 3 h. Then, the mixture was concentrated by the distillation of pyridine at atmospheric pressure to a syrupy consistency. Water (demineralized, approx. 400 mL) was added dropwise at 65–75 °C. The resulting foamy mixture was heated at 95 °C for 1.5 h, then the mixture was cooled to r.t., and the solid product was filtered off and washed with water and EtOH (200 mL). The product was dried under vacuum at 75 °C for a total of 61.7 g and a 76% yield. The analytical sample was crystallized from THF (mp 283–293 °C; UV (MeOH, nm): 274 λ_{\max} , 320 λ_{\max} , 372 sh). MS APCI + *m/z* 227.1 (M + H)⁺, APCI and ES – *m/z* 225.1 (M – H)[–]. ¹H (500 MHz; DMSO-*d*₆): 1.20 (d, *J* = 7.03 Hz, 6H, –CH(CH₃)₂); 3.30 (br s, 1H); 13.33 (br s, 1H); 13.45 (br s, 1H); 13.84 (br s, 1H). ¹³C (125 MHz; DMSO-*d*₆): 21.9; 24.8; 121.5; 133.0; 143.4; 170.1; 175.1.

3-Isopropyl-7-[4-(2-pyridyl)benzyl]amino-1(2)*H*-pyrazolo[4,3-*d*]pyrimidine-5-thiol (3). 4-(2-Pyridyl)benzylamine (2) (26.2 g; 0.14 mol) was dissolved in 2-methoxyethanol (150 mL) at 50 °C, and 3-isopropyl-1(2)*H*-pyrazolo[4,3-*d*]pyrimidine-5,7-dithiol (2) (23 g, 0.10 mol) was added under nitrogen gas. The reaction mixture was then refluxed for 8 h. The product crystallized after slow cooling at r.t. and then at 5–10 °C. The product was filtered off, washed with 2-methoxyethanol and then with THF, and dried under vacuum at 75 °C. The product (30 g) was obtained as nearly white fine-grain crystals with a 78% yield. Titration in AcOH with 0.1 N HClO₄ gave 100% of the product. Analytical samples were crystallized from DMSO/H₂O and dried under vacuum at 75 °C (mp 263–272 °C; UV (MeOH, nm): 255 λ_{\max} , 289 λ_{\max} , 336 λ_{\max}). MS ESI⁺ 377.1 (M + H)⁺, ESI[–] 375.1 (M – H)[–]. ¹H (500 MHz; DMSO-*d*₆): 1.24 (d, *J* = 7.03 Hz, 6H); 3.32 (br s, 1H); 3.45 (br s, 1H); 4.80 (br s, 2H); 7.31–7.33 (m, 1H); 7.46 (bd, *J* = 6.42 Hz, 2H); 7.83–7.86 (m, 1H); 7.91–7.93 (m, 1H); 8.04 (bd, *J* = 7.34 Hz, 2H); 8.64 (bd, *J* = 3.97 Hz, 1H). ¹³C (125 MHz; DMSO-*d*₆): 21.8; 42.5; 54.8; 120.0, 122.4, 126.4, 127.8, 137.0, 149.4, 155.7.

5-[3-(1-Piperazinyl)-2-hydroxy-1-propyl]thio-3-isopropyl-7-[4-(2-pyridyl)benzyl]amino-1(2)*H*-pyrazolo[4,3-*d*]pyrimidine (4.1). The precursor of the synthesis, 3-(4-Boc-piperazin-1-yl)-1,2-epoxypropane, was prepared by equimolar reaction of epichlorohydrin with *N*-Boc-piperazine in acetonitrile in the presence of K₂CO₃ (2 equivalents); the reaction mixture was stirred at 10 °C for 2 days. The crude product (used in subsequent synthesis) was isolated by filtration and then dried under vacuum at a temperature below 45 °C.

The mixture of 3-isopropyl-7-[4-(2-pyridyl)benzyl]amino-1(2)*H*-pyrazolo[4,3-*d*]pyrimidine-5-thiol 3 (380 mg, 1 mmol), tetramethylammonium hydroxide (0.2 mL 25% solution in MeOH), trimethylamine (0.2 mL, 2.2 mmol), and 3-(4-Boc-piperazin-1-yl)-1,2-epoxypropane (0.45 g, 1.8 mmol) in MeOH (5 mL) was stirred at room temperature for 2 days. The crude Boc product was isolated by precipitation after adding water. The precipitate was dissolved in 3 mL trifluoroacetic acid and was left 2 h at room temperature. The solution was evaporated under vacuum, and the product was purified stepwise (5, 8, and 10%) with MeOH in CHCl₃ with a trace amount of aqueous NH₄OH by column chromatography. Chromatography provided (after evaporation under vacuum) an amorphous colorless glass foam (0.25 g, 48% yield). ESI⁺ 519.1 (M + H)⁺, ESI[–] 517.1 (M – H)[–]. ¹H (500 MHz; DMSO-*d*₆): 1.36 (d, *J* = 7.03 Hz, 6H, –CH–CH₃); 1.37 (d, *J* = 7.03 Hz, 6H, –CH–CH₃); 2.33–2.42 (m, 6H, N–

CH₂–CH–OH + 2 × –CH₂–); 2.77–2.79 (m, 4H, 2 × –CH₂–); 3.01 (dd, *J* = 13.45 Hz, *J* = 7.03 Hz, 1H, –S–CH₂H_β–); 3.27 (sept., *J* = 7.03 Hz, 1H, –CH(CH₃)₂); 3.35 (dd, *J* = 13.60 Hz, *J* = 4.58 Hz, 1H, –S–CH₂H_β–); 3.90 (m, 1H, –CH₂–CH–OH); 4.78 (br s, 2H, –NH–CH₂–); 7.33 (qd, *J* = 7.41 Hz, *J* = 4.89 Hz, *J* = 1.22 Hz, 1H, H_{Ar}); 7.49 (d, *J* = 8.25 Hz, 2H, H_{Ar}); 7.86 (td, *J* = 7.95 Hz, *J* = 1.83 Hz, 1H, H_{Ar}); 7.93 (dt, *J* = 8.25 Hz, *J* = 1.1 Hz, 1H, H_{Ar}); 8.06 (d, *J* = 8.25 Hz, 2H, H_{Ar}); 8.34 (br s, 1H, –NH–CH₂–); 8.65 (qd, *J* = 4.86 Hz, *J* = 1.83 Hz, *J* = 0.92 Hz, 1H, H_{Ar}); 12.80 (br s, 1H, –NH–). ¹³C (125 MHz; DMSO-*d*₆): 21.6; 21.7; 25.7; 36.0; 42.9; 44.7; 53.1; 63.9; 67.2; 120.0; 122.4; 126.5; 127.9; 137.1; 137.5; 138.3; 139.8; 149.4; 150.1; 155.7; 157.9; 161.2.

5[3-(4-Morpholinyl)-2-hydroxy-1-propyl]thio-3-Isopropyl-7-[4-(2-pyridyl)benzyl]amino-1(2)*H*-pyrazolo[4,3-*d*]pyrimidine (4.2). 1-Chloro-3-morpholinopropan-2-ol (0.40 g, 2.2 mmol; prepared according to the literature⁴⁴) was added to a mixture of 3-isopropyl-7-[4-(2-pyridyl)benzyl]amino-1(2)*H*-pyrazolo[4,3-*d*]pyrimidine-5-thiol 3 (0.38 g, 1 mmol) and K₂CO₃ (0.17 g) in MeOH (10 mL), and the mixture was stirred at 45 °C for 24 h. The crude product was precipitated by adding water and then purified stepwise (3%, 4 and 5%) with MeOH in CHCl₃ by column chromatography. Chromatography provided (after evaporation under vacuum) an amorphous colorless glass foam (0.31 g, 60% yield). MS ESI⁺ 520.1 (M + H)⁺ 15%, 542.1 (M + Na)⁺ 100%, ESI[–] 518.1 (M – H)[–] 30%, 554.2 (M + Cl)[–] 100%. ¹H (500 MHz; CDCl₃): 1.19–1.21 (m, 6H, –CH(CH₃)₂); 2.31–2.35 (m, 3H, –CH–CH₂H_β–N– + –N–(CH₂H_β)₂–); 2.42–2.46 (m, 2H, –N–(CH₂H_β)₂–); 2.53 (dd, *J* = 12.53 Hz, *J* = 8.56 Hz, 1H, –CH–CH₂H_β–N); 3.11–3.19 (m, 2H, –CH(CH₃)₂ + S–CH₂H_β–CH–); 3.27 (d, *J* = 12.53 Hz, 1H, S–CH₂H_β–CH–); 3.50 (br s, 4H, O–(CH₂)₂–); 4.09–4.10 (m, 1H, –CH₂–CH–CH₂–); 4.65 (br s, 2H, –NH–CH₂–); 7.17 (dd, *J* = 7.18 Hz, *J* = 5.20 Hz, 1H, H_{Ar}); 7.23 (d, *J* = 7.95 Hz, 2H, H_{Ar}); 7.42 (br s, 1H, –NH–); 7.59 (d, *J* = 7.95 Hz, 1H, H_{Ar}); 7.69 (td, *J* = 7.79 Hz, *J* = 1.83 Hz, 1H, H_{Ar}); 7.73 (d, *J* = 7.95 Hz, 2H, H_{Ar}); 8.58 (d, *J* = 4.58 Hz, 1H, H_{Ar}). ¹³C (125 MHz; CDCl₃): 21.5; 21.6; 26.1; 36.3; 44.2; 53.8; 63.9; 66.5; 68.5; 120.7; 122.2; 127.0; 128.1; 137.0; 138.3; 138.6; 149.4; 156.8; 162.9.

5-(1-Hydroxy-2-butyl)thio-3-isopropyl-7-[4-(2-pyridyl)benzyl]amino-1(2)*H*-pyrazolo[4,3-*d*]pyrimidine (4.3). The precursor of the synthesis, 2-bromo-1-butanol, was obtained by introducing diborane gas into a THF solution of 2-bromobutanoic acid at –10 °C for 5 h, then at 0 °C for 5 h, and finally at 25 °C for 2 h. The excess diborane was consumed by adding 50% aq HCOOH, and the mixture was then concentrated by evaporation (15 Torr, 25 °C). The remaining solution was neutralized by aq NaHCO₃, and the product was extracted by EtOAc. The combined organic phase was dried (Na₂SO₄) and evaporated (15 Torr, 25 °C). The crude product (ρ = 1.38 g/mL) was directly used in the subsequent alkylation reaction.

The mixture of 3-isopropyl-7-[4-(2-pyridyl)benzyl]amino-1(2)*H*-pyrazolo[4,3-*d*]pyrimidine-5-thiol 3 (0.225 g, 0.66 mmol), dimethylformamide (DMF; 5 mL), K₂CO₃ (0.2 g), and 2-bromo-1-butanol (120 μ L, 1.0 mmol) was stirred at 50 °C for 8 h. Subsequently, the reaction mixture was evaporated at a temperature below 50 °C, and the residue was partitioned between EtOAc and H₂O. The combined organic phase was dried (MgSO₄) and evaporated under vacuum. The product was finally purified stepwise (2, 3, and 4%) with MeOH in CHCl₃ by column chromatography and was crystallized from absolute Et₂O (0.07 g, 22% yield, mp 126–129 °C). MS ESI⁺ 449.1 (M + H)⁺, ESI[–] 447.1 (M – H)[–]. NMR: ¹H (500 MHz, DMSO-*d*₆): δ 0.96 (t, *J* = 7.4 Hz, 3H, –CH₃); 1.35–1.39 (m, 6H, –CH(CH₃)₂); 1.55–1.63 (m, 1H, –CH₂H_β–CH₃); 1.81–1.88 (m, 1H, –CH₂H_β–CH₃); 3.24 (m, *J* = 6.9 Hz, 1H, –CH(CH₃)₂); 3.50–3.54 (m, 1H, –S–CH–); 3.70–3.75 (m, 2H, –CH₂–OH); 4.77 (t, *J* = 4.9 Hz, 2H, NH–CH₂–); 4.87 (br s, 1H, –OH), 7.32–7.35 (m, 1H, H_{Ar}); 7.45–7.55 (m, 2H, H_{Ar}); 7.85–7.95 (m, 2H, H_{Ar}); 8.00–8.09 (m, 3H, H_{Ar} + –NH); 8.65–8.66 (m, 1H, H_{Ar}); 12.16 (s, 1H, –NH). ¹³C (125 MHz, DMSO-*d*₆): δ 11.3, 21.5, 21.6, 21.7, 23.6, 24.9, 26.3, 40.4, 43.1, 48.5, 63.1, 120.1, 120.4, 122.3, 122.5, 126.3, 126.6, 127.7, 128.0,

130.4, 137.1, 137.6, 138.6, 139.6, 139.9, 140.6, 148.6, 148.7, 149.4, 153.7, 155.6, 155.8, 161.1.

5-(2-Methylthio-1-ethyl)thio-3-isopropyl-7-[4-(2-pyridyl)benzyl]amino-1(2)*H*-pyrazolo[4,3-*d*]pyrimidine (4.4). To a solution of 3-isopropyl-7-[4-(2-pyridyl)benzyl]amino-1(2)*H*-pyrazolo[4,3-*d*]pyrimidine-5-thiol 3 (0.38 g, 1.0 mmol) in DMF (6 mL), K₂CO₃ (0.2 g) and 2-chloroethyl methyl sulfide (101 μL, 1 mmol) were added, and the mixture was stirred at room temperature for 16 h. The reaction mixture was evaporated at a temperature below 50 °C, and the residue was partitioned between CHCl₃ and H₂O. The combined organic phase was dried with sodium sulfate and evaporated under vacuum. The product was purified stepwise (2, 3, and 4%) with MeOH in CHCl₃ by column chromatography, and the product was crystallized from abs. Et₂O (0.35 g, 74% yield, mp 140–141 °C). APCI + 474.3 (M + H)⁺, ESI⁻ 472.2 (M - H)⁻. ¹H (500 MHz; CDCl₃): 1.33 (d, *J* = 7.03 Hz, 6H, -CH(CH₃)₂); 2.12 (s, 3H, -S-CH₃); 2.80–2.83 (m, 2H, H₃C-S-CH₂-); 3.26–3.30 (m, 3H, -S-CH₂- + -CH(CH₃)₂); 4.62 (br s, 2H, -NH-CH₂-); 6.66 (br s, 1H, -NH-CH₂-); 7.15–7.22 (m, 3H, H_{Ar}); 7.61 (d, *J* = 8.25 Hz, 1H, H_{Ar}); 7.70–7.74 (m, 3H, H_{Ar}); 8.59 (d, *J* = 4.89 Hz, 1H, H_{Ar}); 12.13 (br s, 1H, -NH-). ¹³C (125 MHz; CDCl₃): 15.2; 21.6; 26.2; 30.6; 34.0; 44.0; 121.0; 122.4; 127.0; 127.9; 137.2; 138.1; 138.7; 149.3; 157.0; 161.7.

5-(2-Hydroxycyclohexyl)thio-3-isopropyl-7-[4-(2-pyridyl)benzyl]amino-1(2)*H*-pyrazolo[4,3-*d*]pyrimidine (4.5). 1,2-epoxycyclohexane (0.12 mL, 1.15 mmol) in MeOH (2 mL) was added to a stirred mixture of 3-isopropyl-7-[4-(2-pyridyl)benzyl]amino-1(2)*H*-pyrazolo[4,3-*d*]pyrimidine-5-thiol 3 (0.38 g, 1 mmol) and tetramethylammonium hydroxide (catalytic amount, 80 mg) in MeOH (6 mL), and the mixture was stirred at 40 °C for 7 h. The reaction mixture was evaporated at a temperature below 50 °C, and the residue was partitioned between 2-methyltetrahydrofuran and H₂O. The combined organic phase was dried with magnesium sulfate and evaporated under vacuum. The product was purified stepwise (2, 3, and 4%) with MeOH in CHCl₃ by column chromatography. Chromatography provided (after evaporation under vacuum) an amorphous colorless glass foam (0.22 g, 46% yield). MS ESI⁺ 475.1 (M + H)⁺, ESI⁻ 473.1 (M - H)⁻. ¹H (500 MHz; CDCl₃): 1.18 (d, *J* = 7.03 Hz, 3H, -CH₃); 1.20–1.22 (m, 2H, -CH₂H_β-CH₂-CH-S + -CH₂H_β-CH₂-CH-OH); 1.24 (d, *J* = 7.03 Hz, 3H, -CH₃); 1.33–1.40 (m, 2H, -CH₂H_β-CH-S- + -CH₂H_β-CH-OH); 1.68–1.70 (m, 2H, -CH₂H_β-CH₂-CH-S- + -CH₂H_β-CH₂-CH-OH); 2.08–2.17 (m, 2H, -CH₂H_β-CH-S- + -CH₂H_β-CH-OH); 3.19 (sept., *J* = 7.03 Hz, 1H, -CH(CH₃)₂); 3.45 (ddd, *J* = 13.21 Hz, *J* = 10.09 Hz, *J* = 3.97 Hz, 1H, -S-CH₂-); 3.54 (td, *J* = 10.70 Hz, *J* = 4.26 Hz, 1H, -CH-OH); 4.65 (br s, 2H, -NH-CH₂-); 7.17–7.21 (m, 3H, H_{Ar}); 7.32 (br s, 1H, -NH-CH₂-); 7.58 (d, *J* = 7.95 Hz, 1H, H_{Ar}); 7.68–7.72 (m, 3H, H_{Ar}); 8.58 (d, *J* = 4.89 Hz, 1H, H_{Ar}). ¹³C (125 MHz; CDCl₃): 21.3; 21.7; 24.0; 26.0; 26.2; 30.2; 31.6; 36.5; 44.0; 51.2; 77.4; 120.8; 121.1; 127.0; 127.9; 137.0; 138.2; 138.6; 149.3; 157.0; 163.6.

5-(3,3,3-Trifluoro-2-hydroxy-1-propyl)thio-3-isopropyl-7-[4-(2-pyridyl)benzyl]amino-1(2)*H*-pyrazolo[4,3-*d*]pyrimidine (4.6). 2-Bromo-1,1,1-trifluoro-2-propanol (0.11 mL, 1.05 mmol) was added dropwise to a mixture of 3-isopropyl-7-[4-(2-pyridyl)benzyl]amino-1(2)*H*-pyrazolo[4,3-*d*]pyrimidine-5-thiol 3 (0.38 g, 1.0 mmol) in DMF (6 mL) and K₂CO₃ (0.12 g), and the reaction mixture was stirred at room temperature for 4 h. The reaction mixture was evaporated at a temperature below 50 °C, and the residue was partitioned between CHCl₃ and H₂O. The product was purified stepwise (2, 3, and 4%) with MeOH in CHCl₃ by column chromatography. The product was crystallized from DCM (0.15 g, 31% yield, mp 174–177 °C). MS ESI⁺ 489.1 (M + H)⁺, ESI⁻ 487.1 (M - H)⁻. NMR: Two tautomers: 2:1 (integration showed in relative values) ¹H (500 MHz; DMSO-*d*₆): 1.35 (d, *J* = 7.03 Hz, 6H, -CH(CH₃)₂ form I); 1.38 (d, *J* = 7.03 Hz, 6H, -CH(CH₃)₂ form II); 2.83–2.92 (m, 1H, -S-CH₂H_β- form I and II); 3.21–3.27 (m, H, -CH(CH₃)₂, form I and II); 3.62 (d, *J* = 13.75 Hz, 1H, -S-CH₂H_β, form II); 3.68 (dd, *J* = 13.75 Hz, *J* = 2.14 Hz, 1H, -S-CH₂H_β, form I); 4.23 (br s, 1H, S-CH₂-CH- form I and II); 4.72

(d, *J* = 5.81 Hz, 2H, NH-CH₂-, form II); 4.78 (d, *J* = 5.50 Hz, 2H, NH-CH₂-, form I); 6.59 (d, *J* = 6.72 Hz, 1H, CH-OH, form I and II); 7.32–7.35 (m, 1H, H_{Ar}, form I and II); 7.45 (d, *J* = 7.95 Hz, 2H, H_{Ar}, form II); 7.50 (d, *J* = 8.25 Hz, 2H, H_{Ar}, form I); 7.82–7.87 (m, 1H, H_{Ar}, form I and II); 7.90–7.95 (m, 1H, H_{Ar}, form I and II); 8.01 (d, *J* = 7.95 Hz, 2H, H_{Ar}, form II); 8.08–8.10 (m, 3H, H_{Ar} + -NH-CH₂-, form I); 8.64–8.66 (m, 1H, H_{Ar}, form I and II); 8.79 (br s, 1H, -NH-, form I); 13.80 (br s, 1H, -NH-, form II). ¹³C (125 MHz; DMSO-*d*₆): mixture of two forms 21.3; 21.4; 21.5; 25.0; 26.3; 26.4; 31.2; 42.4; 43.1; 67.9 (q, -CF₃, form I); 68.0 (q, -CF₃, form II); 120.0; 120.1; 120.5; 122.3; 122.5; 124.2; 126.3; 126.5; 126.6; 127.6; 128.0; 130.5; 134.8; 137.10; 137.15; 137.2; 137.7; 138.9; 139.3; 139.7; 140.3; 148.8; 149.43; 149.48; 154.0; 155.6; 155.8; 160.0.

5-(Prop-2-en-1-yl)thio-3-Isopropyl-7-[4-(2-pyridyl)benzyl]amino-1(2)*H*-pyrazolo[4,3-*d*]pyrimidine (4.7). A 1 N solution of NaOH (1.4 mL) and allyl bromide (0.13 mL, 1.1 mmol) was added to a suspension of 3-isopropyl-7-[4-(2-pyridyl)benzyl]amino-1(2)*H*-pyrazolo[4,3-*d*]pyrimidine-5-thiol 3 (0.38 g, 1.00 mmol) in H₂O (20 mL), and the mixture was stirred at room temperature for 6 h. The product was filtered off and recrystallized from CHCl₃/Et₂O (0.28 g, 67% yield, mp 148–150 °C). MS ESI⁺ 417.2 (M + H)⁺, ESI⁻ 415.3 (M - H)⁻. ¹H (500 MHz; DMSO-*d*₆): 1.38 (d, *J* = 6.72 Hz, 6H, -CH(CH₃)₂); 3.28 (sept., *J* = 7.03 Hz, 1H, -CH(CH₃)₂); 3.74 (d, *J* = 7.03 Hz, 2H, -S-CH₂-CH); 4.77 (br s, 2H, NH-CH₂-); 5.02 (dd, *J* = 9.78 Hz, *J* = 0.92 Hz, 1H, CH₂H_β=CH-); 5.24 (dd, *J* = 16.96 Hz, *J* = 1.53 Hz, 1H, CH₂H_β=CH-); 5.95 (ddd, *J* = 17.1 Hz, *J* = 10.1 Hz, *J* = 7.03 Hz, 1H, CH₂=CH-CH₂-); 7.32 (ddd, *J* = 7.39 Hz, *J* = 4.89 Hz, *J* = 1.22 Hz, 1H, H_{Ar}); 7.49 (d, *J* = 8.56 Hz, 2H, H_{Ar}); 7.84 (td, *J* = 7.64 Hz, *J* = 1.83 Hz, 1H, H_{Ar}); 7.92 (d, *J* = 7.95 Hz, 1H, H_{Ar}); 8.06 (d, *J* = 8.25 Hz, 2H, H_{Ar}); 8.27 (br s, 1H, -NH-CH₂-); 8.65 (ddd, *J* = 4.86 Hz, *J* = 1.83 Hz, *J* = 0.92 Hz, 1H, H_{Ar}); 12.58 (br s, 1H, -NH-). ¹³C (125 MHz; DMSO-*d*₆): 21.6; 25.8; 33.0; 42.9; 116.7; 120.0; 122.4; 126.5; 127.8; 134.9; 137.1; 137.5; 139.8; 149.4; 155.7; 160.1.

5[3-(Dimethylamino)-1-propyl]thio-3-Isopropyl-7-[4-(2-pyridyl)benzyl]amino-1(2)*H*-pyrazolo[4,3-*d*]pyrimidine (4.8). K₂CO₃ (0.6 g) and 3-chloro-*N,N*-dimethylpropylamine hydrochloride (182 mg, 1.15 mmol) were added to a solution of 3-isopropyl-7-[4-(2-pyridyl)benzyl]amino-1(2)*H*-pyrazolo[4,3-*d*]pyrimidine-5-thiol 3 (0.38 g, 1 mmol) in DMSO (10 mL), and the mixture was stirred at 60 °C for 24 h. The reaction mixture was evaporated at a temperature below 50 °C, and the residue was partitioned between CHCl₃ and H₂O. The product was purified stepwise (5, 8 and 10%) with MeOH in CHCl₃ by column chromatography. Chromatography provided (after evaporation under vacuum) an amorphous colorless glass foam (0.33 g, 72% yield). MS ESI⁺ 231.6 (M + 2H)²⁺ 50%, 462.1 (M + H)⁺ 100%, ESI⁻ 460.1 (M - H)⁻. ¹H (500 MHz; CDCl₃): 1.34 (d, *J* = 6.72 Hz, 6H, -CH(CH₃)₂); 1.92 (pent., *J* = 7.03 Hz, 2H, -CH₂-CH₂-CH₂-); 2.22 (s, 6H, -N(CH₃)₂); 2.44 (t, *J* = 7.34 Hz, 2H, -CH₂-); 3.09 (t, *J* = 7.03 Hz, 2H, -CH₂-); 3.29 (sept., *J* = 6.72 Hz, 1H, -CH(CH₃)₂); 4.68 (br s, 2H, NH-CH₂-); 6.87 (br s, 1H, -NH-); 7.18–7.20 (m, 1H, H_{Ar}); 7.27 (d, *J* = 7.64 Hz, 2H, H_{Ar}); 7.60 (d, *J* = 7.95 Hz, 1H, H_{Ar}); 7.70 (t, *J* = 7.93 Hz, 1H, H_{Ar}); 7.76 (d, *J* = 7.64 Hz, 2H, H_{Ar}); 8.60 (d, *J* = 3.97 Hz, 1H, H_{Ar}). ¹³C (125 MHz; CDCl₃): 21.7; 26.2; 27.4; 28.9; 29.6; 43.9; 45.1; 58.5; 120.8; 122.2; 127.0; 127.9; 137.0; 138.0; 139.0; 149.3; 150.6; 156.9; 162.0.

5-[(2-(Dimethylamino)-1-ethyl)]thio-3-isopropyl-7-[4-(2-pyridyl)benzyl]amino-1(2)*H*-pyrazolo[4,3-*d*]pyrimidine (4.9). K₂CO₃ (0.6 g) and 2-chloro-*N,N*-dimethylethylamine hydrochloride (166 mg, 1.15 mmol) were added to a solution of 3-isopropyl-7-[4-(2-pyridyl)benzyl]amino-1(2)*H*-pyrazolo[4,3-*d*]pyrimidine-5-thiol 3 (0.38 g, 1 mmol) in DMSO (10 mL), and the mixture was stirred at 60 °C for 24 h. The reaction mixture was evaporated at a temperature below 50 °C, and the residue was partitioned between CHCl₃ and H₂O. The product was purified stepwise (5, 8, and 10%) with MeOH in CHCl₃ by column chromatography. Chromatography provided (after evaporation under vacuum) an amorphous colorless glass foam (0.30 g, 67% yield). MS ESI⁺ 224.5 (M+2H)²⁺ 70%, 448.1

(M + H)⁺ 100%, ESI⁻ 446.1 (M - H)⁻. ¹H (500 MHz; CDCl₃): 1.31 (d, *J* = 7.03 Hz, 6H, -CH-(CH₃)₂); 2.24 (s, 6H, 2x -CH₃); 2.66 (t, *J* = 7.64 Hz, 2H, -CH₂-); 3.20 (t, *J* = 7.34, 2H, -CH₂-); 3.27 (sept.; *J* = 7.03 Hz, 1H, -CH-(CH₃)₂); 4.62 (br s, 2H, -NH-CH₂-); 6.97 (br s, 1H, -NH-CH-); 7.15–7.16 (m, 1H, ArH); 7.17 (d, *J* = 7.95 Hz, 2H, ArH); 7.55 (d, *J* = 8.25 Hz, 1H, ArH); 7.66 (dd, *J* = 7.64 Hz, *J* = 1.83 Hz, 1H, ArH); 7.69 (d, *J* = 7.95 Hz, 2H, ArH); 8.55 (d, *J* = 3.97 Hz, 1H, ArH). ¹³C (125 MHz; CDCl₃): 21.6; 26.2; 28.0; 43.9; 44.9; 59.0; 120.8; 122.2; 126.9; 127.9; 137.0; 138.0; 138.9; 149.3; 150.6; 156.9; 161.6.

5-(1-Hydroxy-3-methyl-2-butyl)thio-3-isopropyl-7-[4-(2-pyridyl)benzyl]amino-1(2)*H*-pyrazolo[4,3-*d*]pyrimidine (4.10). The precursor 2-bromo-3-methyl-1-butanol was prepared from 3-methylbutanal by bromination with a bromine–dioxane complex (1:1) according to the literature.⁴⁵ The obtained 2-bromo-3-methylbutanal was then reduced to the desired 2-bromo-3-methyl-1-butanol in the usual manner using NaBH₄ and was used for alkylation without purification.

K₂CO₃ (0.6 g) and 2-bromo-3-methyl-1-butanol (0.25 g, 1.5 mmol) were added to a solution of 3-isopropyl-7-[4-(2-pyridyl)benzyl]amino-1(2)*H*-pyrazolo[4,3-*d*]pyrimidine-5-thiol 3 (0.38 g, 1 mmol) in DMSO (10 mL), and the mixture was stirred at room temperature for 48 h. The reaction mixture was kept at a temperature below 50 °C. The residue was partitioned between CHCl₃ and H₂O, and the product was purified stepwise (2, 3 and 4%) with MeOH in CHCl₃ by column chromatography. Chromatography provided (after evaporation under vacuum) an amorphous colorless glass foam (0.31 g, 67% yield). MS ESI⁺ 463.1 (M + H)⁺, ESI⁻ 461.1 (M - H)⁻. ¹H (500 MHz; CDCl₃): 0.92 (d, *J* = 6.72 Hz, 3H, -CH₃); 0.97 (d, *J* = 6.72 Hz, 3H, -CH₃); 1.23 (d, *J* = 6.72 Hz, 3H, -CH₃); 1.24 (d, *J* = 7.03 Hz, 3H, -CH₃); 1.83 (sex., *J* = 6.72 Hz, 1H, -CH-CH-(CH₃)₂); 3.14–3.27 (m, 3H, -CH(CH₃)₂-CH₂-); 3.68–3.71 (m, 1H, -CH-); 4.66 (br s, 2H, NH-CH₂-); 7.04 (br s, 1H, -NH-CH₂-); 7.18–7.22 (m, 3H, H_{Ar}); 7.61 (d, *J* = 7.95 Hz, 1H, H_{Ar}); 7.70 (dd, *J* = 7.64 Hz, *J* = 1.83 Hz, 1H, H_{Ar}); 7.73 (d, *J* = 7.95 Hz, 2H, H_{Ar}); 8.59 (d, *J* = 4.89 Hz, 1H, H_{Ar}), 11.9 (br s, 1H, -NH-). ¹³C (125 MHz; CDCl₃): 18.0; 18.3; 21.4; 21.6; 26.1; 33.5; 35.7; 44.1; 78.4; 120.9; 122.2; 127.1; 128.0; 137.0; 138.3; 138.6; 149.3; 157.0; 163.7.

5-(Methoxymethyl)thio-3-isopropyl-7-[4-(2-pyridyl)benzyl]amino-1(2)*H*-pyrazolo[4,3-*d*]pyrimidine (4.11). Chloromethyl methyl ether (31 μL, 0.41 mmol) was added to a mixture of 3-isopropyl-7-[4-(2-pyridyl)benzyl]amino-1(2)*H*-pyrazolo[4,3-*d*]pyrimidine-5-thiol 3 (0.14 g, 0.37 mmol) and K₂CO₃ (0.10 g) in DMF (3 mL), and then the mixture was stirred at room temperature for 4 h. The reaction mixture was evaporated at a temperature below 50 °C, and the residue was partitioned between CHCl₃ and H₂O. The product was purified stepwise (1, 2, and 3% MeOH) in CHCl₃ by column chromatography. The product was crystallized from DCM (0.11 g, 70% yield, mp 160–162 °C). MS ESI⁺ 421.1 (M + H)⁺, ESI⁻ 419.1 (M - H)⁻. ¹H (500 MHz; DMSO-*d*₆): mixture of two tautomeric forms. 1.36–1.40 (m, 6H, -CH(CH₃)₂); 3.22–3.29 (m, 4H, -CH(CH₃)₂-CH₃); 4.74–4.81 (m, 2H, NH-CH₂-); 5.31–5.36 (m, 2H, -S-CH₂-); 7.32–7.35 (m, 1H, H_{Ar}); 7.47–7.53 (m, 2H, H_{Ar}); 7.85–7.88 (m, 1H, H_{Ar}); 7.90–7.95 (m, 1H, H_{Ar}); 8.02–8.10 (m, 2H, H_{Ar}); 8.65–8.66 (m, 1H, H_{Ar}); 12.23 (br s, -NH-, form I); 13.81 (br s, -NH-, form II). ¹³C (125 MHz; DMSO-*d*₆): mixture of two tautomeric forms. 21.6; 21.7; 24.8; 26.2; 42.6; 43.2; 55.9; 73.4; 120.0; 120.6; 122.3; 122.4; 126.3; 126.6; 127.6; 128.0; 137.1; 137.7; 139.4; 139.9; 148.7; 148.9; 149.4; 153.9; 155.6; 155.8; 159.2.

5-(2-Hydroxycyclopentyl)thio-3-isopropyl-7-[4-(2-pyridyl)benzyl]amino-1(2)*H*-pyrazolo[4,3-*d*]pyrimidine (4.12). A solution of 1,2-epoxycyclopentane (0.10 mL, 1.15 mmol) in MeOH (2 mL) was added to a stirred mixture of 3-isopropyl-7-[4-(2-pyridyl)benzyl]amino-1(2)*H*-pyrazolo[4,3-*d*]pyrimidine-5-thiol 3 (0.38 g, 1 mmol) and tetramethylammonium hydroxide (catalytic amount, 80 mg) in MeOH (6 mL), and the mixture was stirred at 40 °C for 7 h. The reaction mixture was evaporated at a temperature below 50 °C, and the residue was partitioned between 2-

methyltetrahydrofuran and H₂O. The combined organic phase was dried with magnesium sulfate and evaporated under vacuum. The product was purified stepwise (2, 3, and 4%) with MeOH in CHCl₃ by column chromatography. Crystallization from CHCl₃ gave 0.25 g (54% yield, mp 148–150 °C). MS ESI⁺ 461.1 (M + H)⁺, ESI⁻ 459.1 (M - H)⁻. ¹H (500 MHz; CDCl₃): 1.17 (d, *J* = 6.42 Hz, 3H, -CH₃); 1.20 (d, *J* = 6.72 Hz, 3H, -CH₃); 1.45–1.53 (m, 1H, -S-CH-CH₂H_β-); 1.64–1.78 (m, 3H, -CH₂-CH₂-CH₂- + HO-CH-CH₂H_β-); 2.02–2.12 (m, 2H, -S-CH-CH₂H_β- + HO-CH-CH₂H_β-); 3.17 (sept., *J* = 7.03 Hz, 1H, -CH(CH₃)₂); 3.60–3.65 (m, 1H, -S-CH-CH₂-); 4.20–4.24 (m, 1H, HO-CH-CH₂-); 4.67 (br s, 2H, NH-CH₂-); 7.17–7.25 (m, 3H, H_{Ar}); 7.60 (d, *J* = 7.64 Hz, 1H, H_{Ar}); 7.68–7.74 (m, 3H, H_{Ar}); 8.58–8.59 (m, 1H, H_{Ar}); 12.13 (br s, 1H, NH). ¹³C (125 MHz; CDCl₃): 21.3; 21.8; 22.7; 25.8; 29.7; 34.4; 44.2; 50.6; 82.7; 120.8; 122.3; 127.1; 128.2; 137.0; 138.3; 138.4; 149.3; 156.8; 164.4.

5-(2-Aminocyclohexyl)thio-3-isopropyl-7-[4-(2-pyridyl)benzyl]amino-1(2)*H*-pyrazolo[4,3-*d*]pyrimidine (4.13). 1,2-Cyclohexenimine (0.60 mL, 5 mmol; prepared according to the literature⁴⁶) was added dropwise at room temperature to a stirred mixture of 3-isopropyl-7-[4-(2-pyridyl)benzyl]amino-1(2)*H*-pyrazolo[4,3-*d*]pyrimidine-5-thiol 3 (0.38 g, 1.0 mmol) and 1 mL of aq 48% HBr solution in DMF (10 mL). The mixture was stirred for 24 h. The reaction mixture was then neutralized with an aq solution of Na₂CO₃, and the crude product was isolated as a precipitate. The product was purified, stepwise (5, 8, and 11%) with MeOH in CHCl₃, with a trace amount of aq NH₄OH, by column chromatography. Chromatography provided a product crystallized from CHCl₃ (0.06 g, 13% yield, mp 165–185 °C). MS APCI + 474.4 (M + H)⁺, APCI - 442.2 (M - H)⁻. ¹H (500 MHz; DMSO-*d*₆): 1.15–1.31 (m, 4H, H-cyclohexyl); 1.38 (d, *J* = 7.03 Hz, 6H, -CH(CH₃)₂); 1.44–1.49 (m, 1H, H-cyclohexyl); 1.59–1.67 (m, 1H, H-cyclohexyl); 1.89–1.92 (m, 1H, H-cyclohexyl); 2.20–2.23 (m, 1H, H-cyclohexyl); 2.64 (td, *J* = 10.09 Hz, *J* = 3.97 Hz, 1H, H-cyclohexyl); 3.23–3.28 (m, 3H, -CH(CH₃)₂-CH₂-); 3.36–3.45 (m, 1H, H-cyclohexyl); 4.72–4.81 (m, 2H, NH-CH₂-); 7.33 (ddd, *J* = 7.34 Hz, *J* = 4.86 Hz, *J* = 1.22, 1H, H_{Ar}); 7.48 (d, *J* = 8.25 Hz, 2H, H_{Ar}); 7.86 (td, *J* = 7.34 Hz, *J* = 1.83 Hz, 1H, H_{Ar}); 7.93 (d, *J* = 7.95 Hz, 1H, H_{Ar}); 8.06 (d, *J* = 8.25 Hz, 2H, H_{Ar}); 8.29 (br s, 1H, -NH-); 8.65 (ddd, *J* = 4.89 Hz, *J* = 1.53 Hz, *J* = 0.92 Hz, 1H, H_{Ar}). ¹³C (125 MHz; DMSO-*d*₆): 21.5; 21.6; 24.3; 25.7; 30.6; 32.8; 35.0; 42.9; 52.2; 52.6; 79.1; 120.0; 122.4; 126.5; 127.7; 137.1; 137.4; 139.8; 149.4; 155.7; 160.8.

3-Isopropyl-7-[4-(2-pyridyl)benzyl]amino-5-methylsulfanyl-1(2)*H*-pyrazolo[4,3-*d*]pyrimidine (4.14). This compound was prepared according to the literature.³⁰

5-(2-Acetylamino-1-ethyl)thio-3-isopropyl-7-[4-(2-pyridyl)benzyl]amino-1(2)*H*-pyrazolo[4,3-*d*]pyrimidine (4.15). This compound was isolated by column chromatography as a byproduct of the synthesis of 5-(2-ureido-1-ethyl)thio-3-isopropyl-7-[4-(2-pyridyl)benzyl]amino-1(2)*H*-pyrazolo[4,3-*d*]pyrimidine (4.27). The isolation yielded an amorphous colorless glass foam (0.08 g, 20% yield). MS ESI⁺ 232.5 (M+2H)²⁺ 100%, 463.1 (M + H)⁺ 60%, ESI⁻ 461.1 (M - H)⁻. NMR: mixture of tautomers: ¹H (500 MHz, CDCl₃): δ 1.36 (d, *J* = 7.0 Hz, 6H, -CH(CH₃)₂); 1.77–1.78 (m, 3H, -CH₃); 3.18 (t, *J* = 5.8 Hz, 2H, -CH₂-CH₂-); 3.31 (sept, *J* = 7.0 Hz, 1H, -CH(CH₃)₂); 3.47 (d, *J* = 5.5 Hz, 2H, -CH₂-CH₂-); 4.73 (d, *J* = 3.7 Hz, 2H, NH-CH₂-); 7.08 (br s, 1H, -NH); 7.18–7.21 (m, 1H, H_{Ar}); 7.36 (d, *J* = 8.3 Hz, 2H, H_{Ar}); 7.61 (d, *J* = 7.9 Hz, 1H, H_{Ar}); 7.69–7.73 (m, 1H, H_{Ar}); 7.82 (d, *J* = 8.3 Hz, 2H, H_{Ar}); 8.60 (d, *J* = 4.9 Hz, 1H, H_{Ar}). ¹³C (125 MHz, CDCl₃): 21.8; 23.1; 26.3; 30.3; 40.5; 44.2; 120.7; 122.3; 127.1; 128.1; 137.1; 138.2; 138.8; 149.3; 150.1; 156.7; 161.8; 171.3.

5-(2-Hydroxy-1-butyl)thio-3-isopropyl-7-[4-(2-pyridyl)benzyl]amino-1(2)*H*-pyrazolo[4,3-*d*]pyrimidine (4.16). A solution of 1,2-epoxybutane (0.1 mL, 1.15 mmol) in MeOH (2 mL) was added to a stirred mixture of 3-isopropyl-7-[4-(2-pyridyl)benzyl]amino-1(2)*H*-pyrazolo[4,3-*d*]pyrimidine-5-thiol 3 (0.38 g, 1 mmol) and tetramethylammonium hydroxide (catalytic amount, 60 mg) in MeOH (6 mL), and the mixture was stirred at room temperature for 10 h. The product was precipitated after adding water and then

purified stepwise (1, 2, and 3%) with MeOH in CHCl₃ by column chromatography. Chromatography yielded (after evaporation under vacuum) an amorphous colorless glass foam (0.28 g, 62% yield). MS ESI⁺ 449.2 (M + H)⁺ 20%, 471.3 (M + Na)⁺ 100%, ESI⁻ 447.2 (M - H)⁻. ¹H (500 MHz; CDCl₃): 0.89 (t, J = 7.34 Hz, 3H, -CH₃); 1.18 (d, J = 5.83 Hz, 6H, -CH(CH₃)₂); 1.51–1.66 (m, 2H, -CH-CH₂-CH₃); 3.09 (dd, J = 14.98 Hz, J = 7.03, 1H, -S-CH_αH_βCH-); 3.18 (sept, J = 6.72 Hz, 1H, -CH(CH₃)₂); 3.27 (bd, J = 14.67 Hz, 1H, -S-CH_αH_βCH-); 3.89–3.91 (m, 1H, -CH-OH); 4.64 (br s, 2H, -NH-CH₂-); 7.16–7.19 (m, 3H, H_{Ar}); 7.57 (d, J = 7.95 Hz, 1H, H_{Ar}); 7.67–7.71 (m, 3H, H_{Ar}); 8.56 (d, J = 3.67 Hz, 1H, H_{Ar}). ¹³C (125 MHz; CDCl₃): 9.8; 21.50; 21.56; 26.1; 29.4; 37.6; 44.0; 74.3; 120.9; 122.2; 127.0; 127.9; 137.0; 138.1; 138.5; 149.2; 156.9; 163.5.

5-[2-(1-Imidazolyl)-1-ethyl]thio-3-isopropyl-7-[4-(2-pyridyl)benzyl]amino-1(2)H-pyrazolo[4,3-d]pyrimidine (4.17).

The precursor for synthesis, *N*-(2-chloroethyl)imidazole, was prepared by stirring 20 g sodium imidazolidine in 1,2-dichloroethane (80 mL) at room temperature for 3 days. After adding water, the product was extracted in 1,2-dichloroethane and was then obtained by the evaporation of the organic phase under vacuum (15 Torr). This crude product was used in subsequent synthesis.

K₂CO₃ (0.2 g) and *N*-(2-chloroethyl)imidazole (143 mg, 1.1 mmol) were added to a solution of 3-isopropyl-7-[4-(2-pyridyl)benzyl]amino-1(2)H-pyrazolo[4,3-d]pyrimidine-5-thiol 3 (0.38 g, 1 mmol) in DMF (8 mL), and the reaction mixture was stirred at room temperature for 24 h. The crude product was precipitated by adding water and purified stepwise (3, 4, and 5%) with MeOH in CHCl₃ by column chromatography. The crystallization from CHCl₃ provided a colorless product (0.21 g, 45% yield, mp 208–211 °C). MS ESI⁺ 471.1 (M + H)⁺, ESI⁻ 469.1 (M - H)⁻. NMR: mixture of tautomers, ¹H (500 MHz, DMSO-*d*₆): δ 1.39 (d, J = 6.7 Hz, 6H, -CH(CH₃)₂); 3.29–3.41 (m, 3H, -CH(CH₃)₂ + -CH₂-CH₂-); 4.26 (br s, 2H, -CH₂-CH₂-); 4.75–4.79 (m, 2H, NH-CH₂-); 6.88 (s, 1H, H_{Ar}); 7.17 (s, 1H, H_{Ar}); 7.33 (s, 1H, H_{Ar}); 7.44–7.59 (m, 3H, H_{Ar}); 7.85–8.13 (m, 5H, H_{Ar} + -NH-); 8.65 (s, 1H, H_{Ar}); 12.26 (s, 1H, -NH-). ¹³C (125 MHz, DMSO-*d*₆): δ 21.7; 26.4; 31.1; 42.6; 43.2; 45.7; 119.2; 120.1; 122.5; 126.5; 126.7; 127.5; 128.0; 128.4; 137.2; 137.7; 139.4; 148.8; 149.5; 155.7; 159.7.

5-(3-Amino-2-hydroxy-1-propyl)thio-3-isopropyl-7-[4-(2-pyridyl)benzyl]amino-1(2)H-pyrazolo[4,3-d]pyrimidine (4) (R/S) mixture (4.18) and (R) Antipode (4.31). K₂CO₃ (0.17 g) and 3-benzylidenamino-1-chloropropan-2-ol (0.55 g, 3 mmol; *R* or *R/S* prepared from *R* or *R/S*-epichlorohydrin according to the literature⁴⁷) were added to a solution of 3-isopropyl-7-[4-(2-pyridyl)benzyl]amino-1(2)H-pyrazolo[4,3-d]pyrimidine-5-thiol 3 (0.38 g, 1 mmol) in MeOH (10 mL), and the mixture was stirred at 40 °C for 24 h. The reaction mixture was then acidified by conc. aq HCl and stirred at 45 °C for 5 h. The crude product was concentrated under vacuum, then alkalinized by adding 1 g Na₂CO₃ in 10 mL water, and crystallized from a water solution at 4–8 °C. The product was then purified stepwise (5, 8, and 10%) with MeOH in CHCl₃, with a trace amount of aq NH₄OH, by column chromatography. Crystallization from MeOH afforded the product (0.30 g; 67% yield; mp 124–128 °C, (*R/S*)-antipode; mp 120–125 °C, (*R*)-antipode). MS ESI⁺ 450.1 (M + H)⁺ 100%, 472.1 (M + Na)⁺ 20%, ESI⁻ 448.1 (M - H)⁻, 484.1 (M + Cl)⁻ 40%, α_D (*R*)-antipode = -4.8°, (c 1.37 g/100 mL, DMSO, 22 °C). ¹H (500 MHz; CD₃OD): 1.40 (d, J = 7.03 Hz, 6H, -CH(CH₃)₂); 2.68 (dd, J = 13.14 Hz, J = 7.64 Hz, 1H, NH₂-CH_αH_β-CH); 2.82 (dd, J = 13.14 Hz, J = 3.67 Hz, 1H, NH₂-CH_αH_β-CH); 3.23 (dd, J = 14.37 Hz, J = 6.42 Hz, 1H, -S-CH_αH_β-CH); 3.30 (dd, J = 14.37 Hz, J = 5.50 Hz, 1H, -S-CH_αH_β-CH); 3.38 (sept, J = 7.03 Hz, 1H, -CH(CH₃)₂); 3.87–3.91 (m, 1H, -CH₂-CH₂-); 4.84 (br s, 2H, NH-CH₂-); 7.31 (ddd, J = 7.34 Hz, J = 5.04 Hz, J = 0.92 Hz, 1H, H_{Ar}); 7.49 (d, J = 8.25 Hz, 2H, H_{Ar}); 7.77 (d, J = 8.25 Hz, 1H, H_{Ar}); 7.84 (td, J = 7.49 Hz, J = 1.83 Hz, 1H, H_{Ar}); 7.88 (d, J = 8.25 Hz, 2H, H_{Ar}); 8.56 (d, J = 4.58 Hz, 1H, H_{Ar}). ¹³C (125 MHz; CD₃OD): 22.2; 27.0; 36.1; 44.8; 46.7; 72.7; 122.5; 123.7; 128.3; 128.4; 129.1; 138.9; 139.1; 139.4; 141.0; 150.2; 158.5; 163.9.

5-(2-Hydroxy-2-methyl-1-propyl)thio-3-isopropyl-7-[4-(2-pyridyl)benzyl]amino-1(2)H-pyrazolo[4,3-d]pyrimidine (4.19).

A solution of 1,2-epoxy-2-methylpropane (0.12 mL, 1.3 mmol) in MeOH (2 mL) was added to a stirred mixture of 3-isopropyl-7-[4-(2-pyridyl)benzyl]amino-1(2)H-pyrazolo[4,3-d]pyrimidine-5-thiol 3 (0.38 g, 1 mmol) and tetramethylammonium hydroxide (catalytic amount, 40 mg) in MeOH (6 mL), and the mixture was stirred at room temperature for 7 h. The crude product was isolated as a precipitate after adding water. The product was purified stepwise (2, 3, and 4%) with MeOH in CHCl₃ by column chromatography. Chromatography yielded (after evaporation under vacuum) an amorphous colorless glass foam (0.28 g, 62% yield). MS ESI⁺ 449.1 (M + H)⁺, ESI⁻ 447.1 (M - H)⁻. ¹H (500 MHz; CDCl₃ + drop of DMSO-*d*₆): 1.23 (d, J = 6.72 Hz, 6H, -CH(CH₃)₂); 1.35 (s, 6H, -C(CH₃)₂); 3.18–3.22 (m, 3H, -CH(CH₃)₂, -CH₂-); 4.69 (bd, J = 4.89 Hz, 2H, NH-CH₂-); 7.19 (ddd, J = 7.34 Hz, J = 4.89 Hz, J = 0.92, 1H, H_{Ar}); 7.24 (d, J = 8.25 Hz, 2H, H_{Ar}); 7.27 (br s, 1H, -NH-CH₂-); 7.61 (d, J = 7.95 Hz, 1H, H_{Ar}); 7.71 (td, J = 7.79 Hz, J = 1.83 Hz, 1H, H_{Ar}); 7.75 (d, J = 8.25 Hz, 2H, H_{Ar}); 8.60 (d, J = 4.89 Hz, 1H, H_{Ar}). ¹³C (125 MHz; CDCl₃ + drop of DMSO-*d*₆): 21.5; 26.2; 29.3; 44.0; 44.5; 71.6; 120.8; 122.2; 127.0; 128.0; 137.0; 137.7; 138.3; 138.6; 149.4; 150.2; 157.0; 163.7.

5-(2-Guanidino-1-ethyl)thio-3-isopropyl-7-[4-(2-pyridyl)benzyl]amino-1(2)H-pyrazolo[4,3-d]pyrimidine (4.20).

1*H*-Pyrazole-1-carboxamide hydrochloride (0.143 g, 0.95 mmol) was added to a solution of 5-(2-amino-1-ethyl)thio-3-isopropyl-7-[4-(2-pyridyl)benzyl]amino-1(2)H-pyrazolo[4,3-d]pyrimidine (4.35) (0.35 g, 0.84 mmol) and diethylamine (0.30 mL, 1.7 mmol) in DMF (2 mL), and the reaction mixture was stirred at room temperature for 2 h. The reaction mixture was evaporated at a temperature below 50 °C, and the residue was partitioned between CHCl₃ and H₂O. The combined organic phase was dried with sodium sulfate and evaporated under vacuum. The product was purified stepwise (10, 12, and 14%) with MeOH in CHCl₃, with a trace amount of aq NH₄OH, by column chromatography. Chromatography yielded (after evaporation in vacuo) an amorphous colorless glass foam (0.225 g, 58% yield). MS ESI⁺ 231.7 (M + 2H)²⁺ 100%, 462.1 (M + H)⁺ 30%, ESI⁻ 460.1 (M - H)⁻. NMR: mixture of tautomers: ¹H (500 MHz, DMSO-*d*₆): δ 1.35 (d, J = 7.0 Hz, 6H, -CH(CH₃)₂); 3.16 (d, J = 4.6 Hz, 1H); 3.20 (t, J = 6.3 Hz, 2H, -CH₂-CH₂-); 3.24 (sept, J = 6.9 Hz, 1H, -CH(CH₃)₂); 3.37 (s, 2H); 3.43–3.47 (m, 2H, -CH₂-CH₂-); 4.76 (d, J = 5.2 Hz, 2H, NH-CH₂-); 7.33 (dd, J = 7.0, 5.2 Hz, 1H, H_{Ar}); 7.46 (s, 1H, -NH); 7.50 (d, J = 7.9 Hz, 2H, H_{Ar}); 7.84–7.88 (m, 2H, H_{Ar} + -NH); 7.94 (d, J = 7.9 Hz, 1H, H_{Ar}); 8.06 (d, J = 7.9 Hz, 2H, H_{Ar}); 8.64 (d, J = 4.3 Hz, 1H, H_{Ar}); 8.94 (s, 1H, -NH); 13.05 (s, 1H, -NH). ¹³C (125 MHz, DMSO-*d*₆): δ 21.7; 26.3; 29.4; 40.5; 42.9; 48.6; 120.1; 120.7; 122.5; 126.6; 127.6; 127.8; 137.2; 137.5; 139.7; 139.8; 148.4; 148.9; 149.5; 155.7; 156.9; 159.7.

5-(Carbamoylmethyl)thio-3-isopropyl-7-[4-(2-pyridyl)benzyl]amino-1(2)H-pyrazolo[4,3-d]pyrimidine (4.21).

K₂CO₃ (0.09 g) and 2-chloroacetamide (51 mg, 0.54 mmol) were added to a solution of 3-isopropyl-7-[4-(2-pyridyl)benzyl]amino-1(2)H-pyrazolo[4,3-d]pyrimidine-5-thiol 3 (200 mg, 0.54 mmol) in DMF (6 mL). The reaction mixture was stirred at room temperature for 2 h and evaporated at a temperature below 50 °C. The residue was triturated with water and subsequently crystallized (0.13 g, 56% yield, mp 220–235 °C). MS ESI⁺ 434.2 (M + H)⁺, ESI⁻ 432.3 (M - H)⁻. ¹H (500 MHz; DMSO-*d*₆): 1.36 (d, J = 7.03 Hz, 6H, -CH(CH₃)₂); 3.28 (sept, J = 7.03 Hz, 1H, -CH(CH₃)₂); 3.73 (3H, -S-CH₂-); 4.77 (br s, 2H, -NH-CH₂-); 7.03 (br s, 1H, -C(O)-NH_αH_β); 7.33 (ddd, J = 6.42 Hz, J = 4.89 Hz, J = 0.92 Hz, 1H, H_{Ar}); 7.43 (br s, 1H, -C(O)-NH_αH_β); 7.51 (d, J = 7.95 Hz, 2H, H_{Ar}); 7.88 (td, J = 7.64 Hz, J = 1.53 Hz, 1H, H_{Ar}); 7.93 (d, J = 7.95 Hz, 1H, H_{Ar}); 8.06 (d, J = 7.95 Hz, 2H, H_{Ar}); 8.35 (br s, 1H, -NH-); 8.65 (bd, J = 4.28 Hz, 1H, H_{Ar}). ¹³C (125 MHz; DMSO-*d*₆): 21.6; 25.8; 34.4; 42.9; 120.0; 122.4; 126.5; 128.0; 137.1; 137.5; 139.8; 149.4; 155.7; 160.2; 170.3.

5-(3-Amino-1-propyl)thio-3-isopropyl-7-[4-(2-pyridyl)benzyl]amino-1(2)H-pyrazolo[4,3-d]pyrimidine (4.22). K₂CO₃ (0.35 g) and 3-bromopropylamine hydrochloride (0.40 g, 1.8

mmol) were added to a solution of 3-isopropyl-7-[4-(2-pyridyl)benzyl]amino-1(2)*H*-pyrazolo[4,3-*d*]pyrimidine-5-thiol 3 (0.38 mg, 1 mmol) in DMF (10 mL), and the reaction mixture was stirred at 45 °C for 24 h. DMF was evaporated under vacuum, and the product was purified stepwise (5 and 10%) with MeOH in CHCl₃ with a trace amount of aq NH₄OH by column chromatography. Chromatography yielded (after evaporation under vacuum) an amorphous colorless glass foam (0.30 g, 69% yield). ESI⁺ 434.1 (M + H)⁺, ESI⁻ 432.1 (M - H)⁻. ¹H (500 MHz; DMSO-*d*₆): 1.37 (d, *J* = 7.03 Hz, 6H, -CH-(CH₃)₂); 1.80 (pent., *J* = 7.03 Hz, 2H, -CH₂-CH₂-CH₂-); 2.70 (t, *J* = 7.03 Hz, 2H, -CH₂-); 3.09 (t, *J* = 7.03 Hz, 2H, -CH₂-); 3.27 (sept., *J* = 7.03 Hz, 1H, -CH-(CH₃)₂); 4.77 (br s, 2H, -NH-CH₂-); 7.22 (ddd, *J* = 7.34 Hz, *J* = 4.89 Hz, *J* = 0.92 Hz, 1H, H_{Ar}); 7.48 (d, *J* = 8.56 Hz, 2H, H_{Ar}); 7.85 (dt, *J* = 7.64 Hz, *J* = 1.53 Hz, 1H, H_{Ar}); 7.92 (d, *J* = 7.95 Hz, 1H, H_{Ar}); 8.06 (d, *J* = 8.25 Hz, 2H, H_{Ar}); 8.47 (appt. bt, 1H, -NH-); 8.64 (ddd, *J* = 4.58 Hz, *J* = 1.53 Hz, *J* = 0.92 Hz, 1H, H_{Ar}). ¹³C (125 MHz; DMSO-*d*₆): 21.7; 25.9; 27.5; 31.3; 39.7; 42.9; 120.0; 122.4; 123.3; 126.5; 127.8; 137.1; 137.4; 138.6; 139.9; 145.8; 149.4; 150.2; 155.7; 160.6.

5-(3-Hydroxy-1-propyl)thio-3-isopropyl-7-[4-(2-pyridyl)benzyl]amino-1(2)*H*-pyrazolo[4,3-*d*]pyrimidine (4.23). K₂CO₃ (0.1 g) and 3-bromopropanol (54 μL, 0.6 mmol) were added to a solution of 3-isopropyl-7-[4-(2-pyridyl)benzyl]amino-1(2)*H*-pyrazolo[4,3-*d*]pyrimidine-5-thiol 3 (200 mg, 0.54 mmol) in DMF (6 mL), and the mixture was stirred at room temperature for 3 h. The reaction mixture was evaporated at a temperature below 50 °C, and the residue was partitioned between CHCl₃ and H₂O. The combined organic phase was dried (Na₂SO₄) and evaporated under vacuum. The product was purified stepwise (2, 3, and 4%) with MeOH in CHCl₃ by column chromatography. The product was crystallized from CHCl₃/Et₂O (0.15 g, 66% yield, mp 150–152 °C). MS ESI⁺ 435.2 (M + H)⁺, ESI⁻ 433.3 (M - H)⁻. ¹H (500 MHz; CDCl₃ + DMSO-*d*₆): 1.22 (d, *J* = 7.03 Hz, 6H, -CH(CH₃)₂); 1.72–1.77 (m, 2H, -CH₂-CH₂-CH₂-); 3.14 (t, *J* = 5.50 Hz, 2H, -S-CH₂-); 3.19 (sept., *J* = 7.03 Hz, 1H, -CH(CH₃)₂); 3.50–3.52 (m, 2H, -CH₂-OH); 4.62 (br s, 2H, -NH-CH₂-); 4.77 (br s, 1H, -OH); 7.05–7.07 (m, 1H, H_{Ar}); 7.31 (d, *J* = 7.95 Hz, 2H, H_{Ar}); 7.53–7.59 (m, 3H, H_{Ar} + -NH-CH₂-); 7.81 (d, *J* = 7.03 Hz, 2H, H_{Ar}); 8.47 (d, *J* = 4.58 Hz, 1H, H_{Ar}); 11.66 (br s, 1H, -NH-). ¹³C (125 MHz; CDCl₃ + DMSO-*d*₆): 21.3; 25.7; 26.4; 32.6; 43.7; 58.5; 119.9; 121.8; 126.6; 128.2; 136.4; 138.2; 138.6; 149.1; 156.1; 162.5.

5-(2-Amino-2-methyl-1-propyl)thio-3-isopropyl-7-[4-(2-pyridyl)benzyl]amino-1(2)*H*-pyrazolo[4,3-*d*]pyrimidine (4.24). 2,2-Dimethylaziridine (1.50 mL, 20 mmol; prepared according to the literature⁴⁸) was added dropwise to a stirred mixture of 3-isopropyl-7-[4-(2-pyridyl)benzyl]amino-1(2)*H*-pyrazolo[4,3-*d*]pyrimidine-5-thiol 3 (3.8 g, 10 mmol), DMF (3 mL), aq 48% solution HBr (3 mL), and H₂O (10 mL) at room temperature, and the mixture was stirred for 24 h. The reaction mixture was then neutralized with an aq solution of Na₂CO₃, and the crude product was isolated as a precipitate. The product was purified stepwise (3, 5, 7, and 10%) with MeOH in CHCl₃ with a trace amount of aq NH₄OH by column chromatography. Chromatography yielded (after evaporation under vacuum) an amorphous colorless glass foam (1.6 g, 36% yield). MS ESI⁺ 448.2 (M + H)⁺, ESI⁻ 446.2 (M - H)⁻. NMR: ¹H (500 MHz; DMSO-*d*₆): 1.29 (s, 6H, 2 × -CH₃); 1.33 (d, *J* = 7.03 Hz, 6H, -CH-(CH₃)₂); 3.47 (br s, 1H, -CH-(CH₃)₂); 3.65 (s, 2H, -CH₂-); 5.01 (d, *J* = 5.20 Hz, 2H, -NH-CH₂-); 7.66 (d, *J* = 8.56 Hz, 2H, H_{Ar}); 7.81 (t, *J* = 6.42 Hz, 1H, H_{Ar}); 8.10 (d, *J* = 8.56 Hz, 2H, H_{Ar}); 8.29 (d, *J* = 7.95 Hz, 1H, H_{Ar}); 8.41 (t, *J* = 7.49 Hz, 1H, H_{Ar}); 8.54 (br s, 2H, -NH₂); 8.80 (dd, *J* = 5.2 Hz, *J* = 0.92 Hz, 1H, H_{Ar}). ¹³C (125 MHz; DMSO-*d*₆): 21.8; 24.5; 25.1; 30.7; 34.0; 38.7; 43.5; 48.7; 53.9; 123.8; 124.6; 128.0; 128.2; 132.0; 141.3; 143.6; 144.4; 152.3; 159.7.

5-[(Oxazolidin-2-on-5-yl)methyl]thio-3-isopropyl-7-[4-(2-pyridyl)benzyl]amino-1(2)*H*-pyrazolo[4,3-*d*]pyrimidine (4.25). K₂CO₃ (0.15 g) and 5-chloromethyl-2-oxazolidinone (0.15 g, 1.1 mmol) were added to a solution of 3-isopropyl-7-[4-(2-pyridyl)benzyl]amino-1(2)*H*-pyrazolo[4,3-*d*]pyrimidine-5-thiol 3 (0.38 mg, 1 mmol) in DMF (5 mL), and the reaction mixture was stirred at 45 °C for 24 h. The crude product was precipitated by adding water and

purified stepwise (4, 5, and 6%) with MeOH in CHCl₃ by column chromatography. Chromatography yielded (after evaporation under vacuum) an amorphous colorless glass foam (0.35 g, 74% yield). ESI⁺ 476.2 (M + H)⁺, ESI⁻ 474.2 (M - H)⁻. ¹H (500 MHz; CD₃OD): 1.40 (d, *J* = 7.03 Hz, 6H, -CH(CH₃)₂); 3.28 (dd, *J* = 14.21 Hz, *J* = 7.34 Hz, 1H, -NH-CH₂-CH₂-); 3.35–3.39 (m, 2H, -CH(CH₃)₂ + -S-CH₂-CH₂-); 3.54 (bt, *J* = 8.80 Hz, 1H, -S-CH₂-CH₂-); 3.64 (dd, *J* = 14.06 Hz, *J* = 4.89 Hz, 1H, -NH-CH₂-CH₂-); 4.83 (br s, 2H, NH-CH₂-); 4.85–4.86 (m, 1H, -CH₂-CH₂-); 7.32 (ddd, *J* = 7.47 Hz, *J* = 4.89 Hz, *J* = 1.22 Hz, 1H, H_{Ar}); 7.49 (d, *J* = 8.25 Hz, 2H, H_{Ar}); 7.79 (d, *J* = 7.79 Hz, 1H, H_{Ar}); 7.84 (td, *J* = 7.34 Hz, *J* = 1.83 Hz, 1H, H_{Ar}); 7.89 (d, *J* = 8.25 Hz, 2H, H_{Ar}); 8.56 (d, *J* = 4.89 Hz, 1H, H_{Ar}). ¹³C (125 MHz; CD₃OD): 22.2; 27.1; 35.1; 44.8; 45.7; 77.0; 122.5; 123.6; 128.3; 128.8; 138.8; 139.4; 141.1; 150.2; 158.5; 162.0; 162.4.

5-(2-Carbamoyl-1-ethyl)thio-3-isopropyl-7-[4-(2-pyridyl)benzyl]amino-1(2)*H*-pyrazolo[4,3-*d*]pyrimidine (4.26). K₂CO₃ (0.2 g) and 3-chloropropionamide (65 mg, 0.6 mmol) were added to a solution of 3-isopropyl-7-[4-(2-pyridyl)benzyl]amino-1(2)*H*-pyrazolo[4,3-*d*]pyrimidine-5-thiol 3 (200 mg, 0.54 mmol) in DMF (6 mL). The reaction mixture was then stirred at 50 °C for 8 h. The mixture was evaporated at a temperature below 50 °C, and the residue was partitioned between EtOAc and H₂O. The combined organic phase was dried (Na₂SO₄), and the product was crystallized from EtOAc (0.11 g, 46% yield, mp 137–140 °C). MS ESI⁺ 448.2 (M + H)⁺ 100%, 470.2 (M + Na)⁺ 30%, ESI⁻ 446.3 (M - H)⁻ 100%, 893.3 (2M - H)⁻ 30%. ¹H (500 MHz; DMSO-*d*₆): 1.37 (d, *J* = 7.03 Hz, 6H, -CH(CH₃)₂); 2.51 (t, *J* = 7.03 Hz, 2H, O=C-CH₂-); 3.22 (t, *J* = 7.03 Hz, 2H, -S-CH₂-); 3.27 (sept., *J* = 6.72 Hz, 1H, -CH(CH₃)₂); 4.77 (br s, 2H, -NH-CH₂-); 6.80 (br s, 1H, -C(O)-NH₂-); 7.28 (br s, 1H, -C(O)-NH₂-); 7.32 (ddd, *J* = 7.41 Hz, *J* = 4.74 Hz, *J* = 1.22 Hz, 1H, H_{Ar}); 7.50 (d, *J* = 8.25 Hz, 2H, H_{Ar}); 7.85 (td, *J* = 7.64 Hz, *J* = 1.83 Hz, 1H, H_{Ar}); 7.92 (d, *J* = 7.95 Hz, 1H, H_{Ar}); 8.05 (d, *J* = 8.25 Hz, 2H, H_{Ar}); 8.47 (br s, 1H, -NH₂-); 8.65 (ddd, *J* = 4.89 Hz, *J* = 1.53 Hz, *J* = 0.92 Hz, 1H, H_{Ar}). ¹³C (125 MHz; DMSO-*d*₆): 21.6; 26.0; 35.2; 42.9; 120.0; 122.4; 125.3; 126.5; 127.8; 132.0; 137.1; 137.4; 140.0; 149.4; 155.7; 160.4; 172.7.

5-(2-Ureido-1-ethyl)thio-3-isopropyl-7-[4-(2-pyridyl)benzyl]amino-1(2)*H*-pyrazolo[4,3-*d*]pyrimidine (4.27). A solution of potassium cyanate (0.13 g, 1.6 mmol) in 1 mL of water was added dropwise to a solution of 5-(2-amino-1-ethyl)thio-3-isopropyl-7-[4-(2-pyridyl)benzyl]amino-1(2)*H*-pyrazolo[4,3-*d*]pyrimidine 4.35 (0.35 g, 0.84 mmol) in AcOH (6 mL), and the reaction mixture was stirred at room temperature for 4 h. The reaction mixture was evaporated at a temperature below 50 °C, and the residue was partitioned between CHCl₃ and H₂O. The combined organic phase was dried (Na₂SO₄) and evaporated under vacuum. The product was purified stepwise (3, 5, 7, and 10%) with MeOH in CHCl₃ by column chromatography. Chromatography yielded (after evaporation under vacuum) an amorphous colorless glass foam (0.12 g, 31% yield). MS ESI⁺ 232.5 (M+2H)²⁺ 100%, 463.1 (M + H)⁺ 60%, ESI⁻ 461.1 (M - H)⁻. ¹H NMR (500 MHz, DMSO-*d*₆): δ 1.36 (d, *J* = 6.7 Hz, 6H, -CH(CH₃)₂); 3.04–3.09 (m, 2H, -CH₂-CH₂-); 3.24–3.28 (m, 3H, -CH(CH₃)₂ + -CH₂-CH₂-); 4.78 (s, 2H, NH-CH₂-); 5.49 (s, 2H, -NH₂); 6.16 (br s, 1H, -NH-); 7.33–7.35 (m, 1H, H_{Ar}); 7.52 (d, *J* = 7.3 Hz, 2H, H_{Ar}); 7.87 (t, *J* = 7.0 Hz, 1H, H_{Ar}); 7.94–7.96 (m, 1H, H_{Ar}); 8.08 (d, *J* = 6.7 Hz, 2H, H_{Ar}); 8.65 (s, 1H, H_{Ar}); 12.21 (s, 1H, -NH). ¹³C NMR (125 MHz, DMSO-*d*₆) 21.7; 26.3; 31.0; 35.8; 43.2; 62.8; 79.2; 120.1; 122.5; 126.6; 128.1; 137.2; 139.6; 148.8; 149.5; 155.7; 158.5; 160.4.

5-(3-Methylamino-1-ethyl)thio-3-isopropyl-7-[4-(2-pyridyl)benzyl]amino-1(2)*H*-pyrazolo[4,3-*d*]pyrimidine (4.28). 2-Bromo-*N*-methylethylamine hydrobromide (0.66 g, 3.0 mmol; prepared according to the literature⁴⁹) was added to a mixture of 3-isopropyl-7-[4-(2-pyridyl)benzyl]amino-1(2)*H*-pyrazolo[4,3-*d*]pyrimidine-5-thiol 3 (0.38 g, 1.0 mmol) in DMF (8 mL) and NaHCO₃ (0.50 g), and the reaction mixture was stirred at room temperature for 2 days. The reaction mixture was evaporated at a temperature below 50 °C, and the residue was partitioned between

CHCl₃ and H₂O. The combined organic phase was dried (Na₂SO₄) and evaporated under vacuum. The product was purified stepwise (6, 8, and 10%) with MeOH in CHCl₃ with a trace amount of aq NH₄OH by column chromatography. Chromatography yielded (after evaporation under vacuum) an amorphous colorless glass foam (0.07 g, 16% yield). MS ESI⁺ 434.1 (M + H)⁺, ESI⁻ 432.1 (M - H)⁻. ¹H (500 MHz; CDCl₃): δ 1.30 (d, J = 7.0 Hz, 6H, -CH(CH₃)₂); 2.42 (s, 3H, -NH-CH₃); 3.00 (t, J = 6.0 Hz, 2H, -CH₂-CH₂-); 3.22 (m, 3H, -CH(CH₃)₂ + -CH₂-CH₂-); 4.65 (s, 2H, NH-CH₂-); 7.16 (ddd, J = 7.34 Hz, J = 4.89 Hz, J = 0.92 Hz, 1H, H_{Ar}); 7.29 (d, J = 8.3 Hz, 2H, H_{Ar}); 7.43 (br s, 1H, -NH); 7.56 (d, J = 7.9 Hz, 1H, H_{Ar}); 7.67 (td, J = 7.7 Hz, J = 1.6 Hz, 1H, H_{Ar}); 7.74 (d, J = 8.1 Hz, 2H, H_{Ar}); 8.59 (d, J = 4.6 Hz, 1H, H_{Ar}). ¹³C (125 MHz; CDCl₃): δ 21.5; 21.7; 26.2; 29.4; 34.7; 44.0; 50.7; 120.7; 122.2; 127.0; 127.8; 128.0; 137.0; 138.1; 138.6; 139.0; 149.3; 150.4; 156.9; 161.2.

5-(2-Hydroxy-1-propyl)thio-3-isopropyl-7-[4-(2-pyridyl)benzyl]amino-1(2)H-pyrazolo[4,3-d]pyrimidine (4.29). A methyloxirane solution (110 mg, 1.8 mmol) in MeOH (2 mL) was added to a stirred mixture of 3-isopropyl-7-[4-(2-pyridyl)benzyl]amino-1(2)H-pyrazolo[4,3-d]pyrimidine-5-thiol 3 (0.38 g, 1 mmol) and tetramethylammonium hydroxide (catalytic amount, 40 mg) in MeOH (6 mL), and the mixture was stirred at room temperature for 6 h. The product was precipitated after adding water, and it was finally purified stepwise (1, 2, and 3%) with MeOH in CHCl₃ by column chromatography. The product was crystallized from DCM/Et₂O (0.30 g, 69% yield, mp 144–146 °C). MS ESI⁺ 435.2 (M + H)⁺, ESI⁻ 433.3 (M - H)⁻. ¹H (500 MHz; CDCl₃): 1.21 (d, J = 6.11 Hz, 6H, -CH(CH₃)₂); 1.25 (d, J = 6.42 Hz, 3H, -CH₃); 3.06 (dd, J = 14.98 Hz, J = 6.72 Hz, -S-CH₂H_β); 3.18 (sept., J = 7.03 Hz, 1H, -CH(CH₃)₂); 3.25 (d, J = 14.37 Hz, 1H, -S-CH₂H_β); 4.19–4.22 (m, 1H, CHOH); 4.67 (br s, 2H, -NH-CH₂-); 7.18–7.23 (m, 3H, H_{Ar}); 7.58 (d, J = 7.95 Hz, 1H, H_{Ar}); 7.69–7.72 (m, 3H, H_{Ar}); 8.59 (d, J = 4.89 Hz, 1H, H_{Ar}). ¹³C (125 MHz; CDCl₃): 21.5; 21.6; 22.7; 26.1; 39.8; 44.0; 69.0; 120.9; 122.3; 127.0; 128.0; 137.1; 138.1; 138.5; 149.2; 156.9; 163.4.

5-(2,3-Diamino-1-propyl)thio-3-isopropyl-7-[4-(2-pyridyl)benzyl]amino-1(2)H-pyrazolo[4,3-d]pyrimidine (4.30). K₂CO₃ (0.15 g) and 2,3-di[(benzyloxycarbonyl)amino]-1-chloropropan (0.41 g, 1.1 mmol) were added to a solution of 3-isopropyl-7-[4-(2-pyridyl)benzyl]amino-1(2)H-pyrazolo[4,3-d]pyrimidine-5-thiol 3 (0.38 g, 1 mmol) in DMF (5 mL). The crude di-Z-protected product was isolated as a precipitate after adding water and then was triturated with 33% HBr in AcOH (1 mL) at room temperature for 1 h. After evaporation under vacuum, the product was purified stepwise (10, 12, and 15%) with MeOH in CHCl₃ with a trace amount of aq NH₄OH by column chromatography. Chromatography yielded (after evaporation under vacuum) an amorphous colorless glass foam (0.31 g, 69% yield). MS ESI⁺ 449.1 (M + H)⁺, ESI⁻ 447.1 (M - H)⁻. ¹H (500 MHz; CDCl₃): 1.30 (d, J = 6.72 Hz, 6H, -CH(CH₃)₂); 2.51 (dd, J = 12.69 Hz, J = 7.03 Hz, 1H, NH₂-CH₂H_β-CH-); 2.75 (dd, J = 12.69 Hz, J = 3.67 Hz, 1H, NH₂-CH₂H_β-CH-); 2.94–3.01 (m, 2H, -S-CH₂H_β-CH- + -S-CH₂-CH-CH₂-); 3.21–3.28 (m, 2H, -CH(CH₃)₂ + -S-CH₂H_β-CH-); 3.80 (br s, 4H, 2 × -NH₂); 4.62 (br s, 2H, -NH-CH₂-); 7.16 (ddd, J = 7.34 Hz, J = 4.89 Hz, J = 0.92 Hz, 1H, H_{Ar}); 7.22 (d, J = 8.25 Hz, 2H, H_{Ar}); 7.27 (br s, 1H, -NH-CH₂-); 7.58 (d, J = 7.95 Hz, 1H, H_{Ar}); 7.67 (td, J = 7.95 Hz, J = 1.83 Hz, 1H, H_{Ar}); 7.75 (d, J = 8.25 Hz, 2H, H_{Ar}); 8.58 (d, J = 4.89 Hz, 1H, H_{Ar}). ¹³C (125 MHz; CDCl₃): 21.7; 21.8; 26.2; 36.6; 43.9; 46.6; 53.2; 120.7; 122.2; 124.8; 127.1; 127.8; 137.0; 138.2; 138.9; 139.0; 146.6; 149.4; 150.8; 156.8; 161.4.

5-(2,3-Dihydroxy-1-propyl)thio-3-isopropyl-7-[4-(2-pyridyl)benzyl]amino-1(2)H-pyrazolo[4,3-d]pyrimidine (4.32). 3-Chloro-1,2-propanediol (0.13 mL, 1.5 mmol) was added to a solution of 3-isopropyl-7-[4-(2-pyridyl)benzyl]amino-1(2)H-pyrazolo[4,3-d]pyrimidine-5-thiol 3 (0.38 g, 1 mmol) in DMF (3 mL) and tetramethylammonium hydroxide (0.11 g), and the mixture was stirred at room temperature for 24 h. The crude product was precipitated after adding water. Then, the mixture was purified stepwise (2, 3, 4, and 5%) with MeOH in CHCl₃ by column chromatography. Chromatography yielded (after evaporation under

vacuum) an amorphous colorless glass foam (0.24 g, 54% yield). MS ESI⁺ 451.1 (M + H)⁺ 100%, 473.2 (M + Na)⁺ 30%, ESI⁻ 449.2 (M - H)⁻. ¹H (500 MHz; CDCl₃ + drop of CD₃OD): 1.32 (d, J = 7.03 Hz, 6H, -CH(CH₃)₂); 3.24–3.31 (m, 3H, -CH(CH₃)₂, -CH₂-); 3.59 (dd, 1H, J = 11.62 Hz, J = 4.89 Hz, -CH₂H_β-); 3.65 (dd, 1H, J = 11.62 Hz, J = 4.89 Hz, -CH₂H_β-); 3.96 (pent., J = 5.20 Hz, 1H, -CH-); 4.71 (br s, 2H, NH-CH₂-); 7.22 (dd, J = 7.03 Hz, J = 5.20 Hz, 1H, H_{Ar}); 7.35 (d, J = 7.95 Hz, 2H, H_{Ar}); 7.63 (d, J = 7.03 Hz, 1H, H_{Ar}); 7.73 (dd, J = 7.34 Hz, J = 1.54 Hz, 1H, H_{Ar}); 7.77 (d, J = 8.25 Hz, 2H, H_{Ar}); 8.58 (d, J = 4.58 Hz, 1H, H_{Ar}). ¹³C (125 MHz; CDCl₃ + drop of CD₃OD): 21.4; 21.5; 25.9; 34.1; 44.1; 64.4; 72.5; 121.1; 122.3; 127.2; 128.3; 137.3; 138.3; 138.6; 149.1; 157.0; 163.4.

5-(2-Hydroxy-1-ethyl)thio-3-isopropyl-7-[4-(2-pyridyl)benzyl]amino-1(2)H-pyrazolo[4,3-d]pyrimidine (4.33). (a) K₂CO₃ (0.2 g) and 2-bromoethanol (45 μL, 0.6 mmol) were added to a solution of 3-isopropyl-7-[4-(2-pyridyl)benzyl]amino-1(2)H-pyrazolo[4,3-d]pyrimidine-5-thiol 3 (200 mg, 0.54 mmol) in DMF (6 mL), and the mixture was stirred at room temperature for 1 h. The reaction mixture was evaporated at a temperature below 50 °C, and the residue was partitioned between CHCl₃ and H₂O. The combined organic phase was dried (Na₂SO₄) and evaporated in vacuo. The product was crystallized from CHCl₃/Et₂O (0.18 g, 80% yield).

(b) A solution of oxirane (80 mg, 1.8 mmol) in 2 mL MeOH was added to a stirred mixture of 3-isopropyl-7-[4-(2-pyridyl)benzyl]amino-1(2)H-pyrazolo[4,3-d]pyrimidine-5-thiol 3 (0.38 g, 1 mmol) and tetramethylammonium hydroxide (catalytic amount, 40 mg) in MeOH (6 mL), and the mixture was stirred for 16 h at room temperature. The product was isolated as a precipitate after adding water. The product was crystallized from CHCl₃/Et₂O (0.36 g, 86% yield).

The analytical sample was recrystallized with the same procedure (mp 145–150 °C; UV (MeOH, nm): 246 λ_{max}, 275 sh 316 sh). MS ESI⁺ 443.2 (M + Na)⁺, ESI⁻ 419.3 (M - H)⁻. ¹H (500 MHz; CDCl₃): 1.23 (d, J = 7.03 Hz, 6H, -CH(CH₃)₂); 3.12–3.16 (m, 2H, -CH₂-); 3.19 (sept., J = 7.03 Hz, 1H, -CH(CH₃)₂); 3.80–3.81 (m, 2H, -CH₂-); 4.63 (br s, 2H, NH-CH₂-); 7.06–7.08 (m, 1H, H_{Ar}); 7.31 (d, J = 8.25 Hz, 2H, H_{Ar}); 7.47 (br s, 1H, -NH-); 7.54–7.61 (m, 2H, H_{Ar}); 7.81 (d, J = 8.25 Hz, 2H, H_{Ar}); 8.48–8.49 (m, 1H, H_{Ar}); 11.71 (br s, 1H, -NH-). ¹³C (125 MHz; CDCl₃): 21.3; 26.0; 33.9; 43.8; 63.5; 119.9; 121.9; 126.6; 128.2; 136.5; 138.3; 138.6; 149.2; 156.1; 162.0.

5-(3-Hydroxy-2-butyl)thio-3-isopropyl-7-[4-(2-pyridyl)benzyl]amino-1(2)H-pyrazolo[4,3-d]pyrimidine (4.34). An E/Z-2,3-dimethyloxirane solution (130 mg, 1.8 mmol, in MeOH, 2 mL) was added to a stirred mixture of 3-isopropyl-7-[4-(2-pyridyl)benzyl]amino-1(2)H-pyrazolo[4,3-d]pyrimidine-5-thiol 3 (0.38 g, 1 mmol) and tetramethylammonium hydroxide (catalytic amount, 40 mg) in MeOH (6 mL), and the mixture was stirred at room temperature for 16 h. The product was precipitated after adding water, and it was finally purified stepwise (1, 2, and 3%) with MeOH in CHCl₃ by column chromatography. The product was crystallized from DCM/Et₂O (0.25 g, 54% yield, mp 168–172 °C). MS ESI⁺ 449.2 (M + H)⁺, ESI⁻ 447.3 (M - H)⁻. ¹H (500 MHz; CDCl₃): δ 1.26–1.29 (m, 6H, -CH-(CH₃)₂); 1.33 (d, J = 6.4 Hz, 3H, -CH-CH₃); 1.43 (d, J = 7.0 Hz, 3H, -CH-CH₃); 3.23 (sept., 1H, -CH-(CH₃)₂); 3.53 (dq, J = 7.03 Hz, J = 7.03 Hz, 1H, -CH-CH₃); 3.90 (dq, J = 6.11 Hz, J = 6.11 Hz, 1H, -CH-CH₃); 4.72 (br s, 2H, NH-CH₂-); 7.20–7.23 (m, 1H, H_{Ar}); 7.25–7.29 (m, 2H, H_{Ar}); 7.64 (d, J = 7.9 Hz, 1H, H_{Ar}); 7.73 (td, J = 7.7, 1.7 Hz, 1H, H_{Ar}); 7.76–7.78 (m, 3H, H_{Ar} + NH-CH₂-); 8.64 (d, J = 4.9 Hz, 1H, H_{Ar}); 11.75 (br s, 1H, -NH). ¹³C (125 MHz; CDCl₃ + DMSO-d₆): δ 17.5; 21.4; 21.5; 21.7; 26.1; 44.0; 48.3; 71.9; 120.1; 122.0; 126.8; 128.3; 136.6; 138.3; 138.6; 149.3; 156.3; 161.8.

5-(2-Amino-1-ethyl)thio-3-isopropyl-7-[4-(2-pyridyl)benzyl]amino-1(2)H-pyrazolo[4,3-d]pyrimidine (4.35). (a) Aziridine (0.42 mL, 8 mmol) was added dropwise to a stirred mixture of 3-isopropyl-7-[4-(2-pyridyl)benzyl]amino-1(2)H-pyrazolo[4,3-d]pyrimidine-5-thiol 3 (1.0 g, 2.66 mmol) and aq 48% solution HBr (3.1 mL) in DMF (20 mL), and the mixture was stirred at room temperature for 24 h. The reaction mixture was neutralized with an aq

solution of Na_2CO_3 , and the crude product was isolated as a precipitate.

(b) 2-(Boc-amino)ethyl bromide (0.61 g, 2.71 mmol) was added to a solution of 3-isopropyl-7-[4-(2-pyridyl)benzyl]amino-1(2)*H*-pyrazolo[4,3-*d*]pyrimidine-5-thiol **3** (1 g, 2.66 mmol) in DMF (30 mL) with K_2CO_3 (0.5 g). The reaction mixture was stirred at room temperature for 16 h. The product was isolated as a precipitate after adding water. The precipitate was dissolved in 25 mL of 2 N aq HCl, and the de-Bocylation reaction was conducted overnight at room temperature. The reaction mixture was neutralized with an aq solution of Na_2CO_3 , and the crude product was isolated as a precipitate.

The product was purified stepwise (3, 5, 7, and 10%) with MeOH in CHCl_3 with a trace amount of aq NH_4OH by column chromatography. Chromatography yielded (after evaporation under vacuum) an amorphous colorless glass foam (process a: 0.72 g, 65% yield; process b: 0.75 g; 67% yield). MS ESI⁺ 420.2 ($\text{M} + \text{H}$)⁺ 100%, 839.3 ($2\text{M} + \text{H}$)⁺ 15%, ESI⁻ 418.2 ($\text{M} - \text{H}$)⁻. ¹H (500 MHz; DMSO-*d*₆): 1.37 (d, *J* = 7.03 Hz, 6H, $-\text{CH}(\text{CH}_3)_2$); 2.90 (t, *J* = 6.72 Hz, 2H, NH_2-CH_2-); 3.13 (t, *J* = 6.72 Hz, 2H, $-\text{CH}_2-\text{S}-$); 3.28 (sept., *J* = 7.03 Hz, 1H, $-\text{CH}(\text{CH}_3)_2$); 4.77 (br s, 2H, $\text{NH}-\text{CH}_2-$); 7.32 (ddd, *J* = 7.34 Hz, *J* = 4.89 Hz, *J* = 0.92 Hz, 1H, H_{Ar}); 7.49 (d, *J* = 8.25 Hz, 2H, H_{Ar}); 7.85 (td, *J* = 7.95 Hz, *J* = 1.83 Hz, 1H, H_{Ar}); 7.92 (d, *J* = 8.25 Hz, 1H, H_{Ar}); 8.06 (d, *J* = 8.25 Hz, 2H, H_{Ar}); 8.47 (bt, *J* = 5.81 Hz, 1H, $-\text{NH}-\text{CH}_2-$); 8.65 (ddd, *J* = 4.74 Hz, *J* = 1.53 Hz, *J* = 0.92 Hz, 1H, H_{Ar}). ¹³C (125 MHz; DMSO-*d*₆): 21.6; 25.8; 32.7; 40.9; 42.9; 120.0; 122.4; 126.5; 127.8; 137.1; 137.4; 138.5; 139.9; 149.4; 155.7; 160.3.

Kinase Inhibition Assay. CDK/cyclin complexes were assayed as previously described.⁵⁰

Protein Crystallization, Diffraction Data Collection, and Structure Determination.

The protein sample for crystallization was prepared by mixing 12 mg/mL CDK2/cycA2 complex in 40 mM 4-(2-hydroxyethyl)-1-piperazineethanesulfonic acid at pH 7.5, 200 mM NaCl, and 0.02% monothio glycerol with 100 mM **4.35** in DMSO to the final inhibitor concentration of 2 mM, followed by 30 min of incubation on ice and purification by centrifugation (16 000g, 10 min, 4 °C). The CDK2/cycA2 crystal in complex with the inhibitor **4.35** was obtained at 18 °C using the sitting-drop vapor diffusion technique and condition no. 21 from the Morpheus kit (Molecular Dimensions, USA), containing 10% w/v polyethylene glycol (PEG) 20 000, 20% v/v PEG MME 550, 0.03 M sodium fluoride, 0.03 M sodium bromide, 0.03 M sodium iodide, and 0.1 M bicine/Trizma base at pH 8.5. The droplet contained 100 nL of the protein sample, 170 nL of the reservoir solution, and 30 nL of a seed stock prepared by crushing crystals prepared in condition no. 93 from the Morpheus kit (Molecular Dimensions, USA) in 30 μL of the precipitant solution, which contained 10% w/v PEG 20 000, 20% v/v PEG MME 550, 0.02 M 1,6-hexanediol, 0.02 M 1-butanol, 0.02 M (RS)-1,2-propanediol, 0.02 M 2-propanol, 0.02 M 1,4-butanediol, 0.02 M 1,3-propanediol, and 0.1 M bicine/Trizma base at pH 8.5. The crystal was harvested after 3 weeks and flash-cooled in liquid nitrogen without additional cryoprotection. A complete data set at 2.15 Å resolution was collected at 100 K at the beamline MX14.1 of BESSY, Berlin, Germany.⁵¹ The data set was processed using the program XDS⁵² and its graphical interface XDSGUI.⁵³ The structure was determined by molecular replacement with the program Molrep⁵⁴ using the structure of CDK2/cycA2 available in the PDB under the code 5LMK⁵⁵ as a search model. Model refinement was performed using the program REFMAC 5.8.0158⁵⁶ from the CCP4 package⁵⁷ in combination with manual adjustments with Coot software.⁵⁸ MolProbability server⁵⁹ was used to evaluate the final model quality. The data collection and refinement statistics are listed in Table S1. All the figures representing structures were created using PyMOL.⁶⁰ Atomic coordinates and structure factors were deposited in the PDB under the accession code 6GVA.

Cell Culture. Lymphoma cell lines were obtained from the German Collection of Microorganisms and Cell Cultures (DSMZ), American Tissue Culture Collection (ATCC) or European Collection of Authenticated Cell Cultures and cultured in media according to providers' instructions. HBL2 cells were kindly provided by Prof.

Martin Dreyling from the University of Munich, Germany. UPF1H and UPF7U are a mantle cell lymphoma cell lines derived by Dr. Pavel Klener (Institute of Pathological Physiology, First Faculty of Medicine, Charles University, Czech Republic). UPF1H was established from the peripheral blood of a patient with treatment-refractory mantle cell lymphoma. Whole exome sequencing confirmed the clonal identity of UPF1H cells to patient lymphoma cells. UPF7U was derived from leukemized blood of a patient with second relapse of mantle cell lymphoma after failure of ibrutinib. Exome sequencing confirmed that UPF7U kept majority of somatic mutations with the primary lymphoma cells, from which it was derived.

Cell Viability Assays. For the viability assays, cells were treated in triplicate with six different doses of each compound for 72 h. After treatments, calcein AM solution was added for 1 h, and the fluorescence of live cells was measured at 485 nm/538 nm (excitation/emission) using a Fluoroskan Ascent microplate reader (Labsystems). The GI₅₀ value, the drug concentration lethal to 50% of the cells, was calculated from the dose response curves that resulted from the assays.

Chemicals. Dinaciclib, venetoclax, and ibrutinib were purchased from MedChemExpress, and CR8 was purchased from Merck.

Immunoblotting. Cell lysates were prepared, and then proteins were separated on sodium dodecyl sulfate-polyacrylamide gels and electroblotted onto nitrocellulose membranes. After blocking, overnight incubation with specific primary antibodies, and incubation with peroxidase-conjugated secondary antibodies, the peroxidase activity was detected with SuperSignal West Pico reagents (Thermo Scientific) using a CCD camera LAS-4000 (Fujifilm). The specific antibodies were purchased from Cell Signaling (anti-PARP, clone 46D11; anti-caspase-7; anti-caspase-3, clone 3G2; anti-Mcl-1, clone D35A5; anti-XIAP; anti-Bcl-xl, clone 54H6; anti-Rb, clone 4H1; anti-pRb S780, clone D59B7; anti-Rb S807/811, clone D20B12; anti-cleaved caspase-9 Asp330; anti-Bax, clone D2E11), Merck (anti-Bcl-2; anti-α-tubulin, clone DM1A), Santa Cruz Biotechnology (anti-β-actin, clone C4; anti-c-myc, clone 9E10), Bethyl Laboratories, USA (anti-phospho-RNA polymerase II S2 and S5), and Millipore (anti-RNA polymerase II, clone ARNA-3). The anti-PCNA (clone PC-10) antibody was generously gifted by Dr. B. Vojtěšek (Masaryk Memorial Cancer Institute, Brno, Czech Republic). All primary antibodies were diluted in phosphate-buffered saline (PBS) containing 5% powdered milk and 0.1% Tween 20. Peroxidase-conjugated rabbit anti-mouse immunoglobulin or porcine anti-rabbit immunoglobulin antisera (Cell Signaling) were used as the secondary antibodies.

In Vivo Efficacy. All aspects of the animal study met the accepted criteria for the care and experimental use of laboratory animals. The protocols were reviewed by the Institutional Animal Care and Use Committee and approved by the Ministry of Education, Youth and Sports of the Czech Republic under number 2844/2017-2. Immunodeficient NOD.Cg-Prkdcscid Il2rgtm1Wjl/SzJ mice (Jackson Laboratory, referred to as "NOD-SCID-gamma" or "NSG" mice) were maintained in individually ventilated cages. The cells were injected sc (5–10 mil. per mouse) into 8–12 week old female NSG mice; numbers of experimental animals are indicated in the legends to Figures 4 and 6. Compound **4.35** dissolved in PBS was administered iv via the tail vein. Therapy was initiated when all animals developed palpable tumors. Tumors were measured every day in two perpendicular dimensions with a digital caliper. In vivo experiments were terminated when at least one mouse in any group developed a sc tumor ≥ 2 cm in any diameter. For the analysis of pharmacodynamic markers, palpable tumor-bearing mice were injected with different doses of **4.35** (5 and 10 mg/kg) and euthanized after 24 h. Subsequently, tumors were excised, filtered through 45 μm nylon mesh, and evaluated for protein expression by immunoblotting analysis.

■ ASSOCIATED CONTENT

Supporting Information

The Supporting Information is available free of charge on the ACS Publications website at DOI: 10.1021/acs.jmedchem.9b00189.

Computational analysis of compound binding to CDK2, crystal parameters and refinement statistics, kinase selectivity profile of **4.35**, NCI60 screening results, additional in vitro data, physicochemical and pharmacological properties of **4.35**, additional in vivo data, additional methods, NMR spectra of prepared compounds, and supplementary references (PDF)

Molecular formula strings (CSV)

Accession Codes

PDB ID Code: 6GVA (complex of **4.35** with CDK2/cyclin A2). Authors will release the atomic coordinates and experimental data upon article publication.

■ AUTHOR INFORMATION

Corresponding Author

*E-mail: vladimir.krystof@upol.cz. Phone: +420585634854.

ORCID

Radek Jorda: 0000-0002-4905-7126

Michaela Nekardová: 0000-0001-5810-7650

Tomáš Pospíšil: 0000-0003-3634-828X

Vladimír Krystof: 0000-0001-5838-2118

Author Contributions

R.J. and L.H. contributed equally; L.H., T.P. and A.Š. prepared and characterized compounds, R.J., D.T., M.A. and M.P. performed biochemical and cellular experiments, P.K., D.T. and L.D. performed animal experiments, Jitka Šíroková and L.U. performed PK analyses, Jana Škerlová, P.P. and P.Ř. performed crystallographic experiments, M.N. performed computational study, R.J., P.K., M.S., and V.K. designed the study, analyzed data and drafted the manuscript.

Notes

The authors declare no competing financial interest.

■ ACKNOWLEDGMENTS

The authors wish to acknowledge the support from the Czech Science Foundation (17-14007S, P208/12/G016), Palacký University in Olomouc (IGA_PrF_2019_013), Charles University (UNCE/MED/016, SVV 260265/2016), and the European Regional Development Fund (Project ENOCH, no. CZ.02.1.01/0.0/0.0/16_019/0000868). The use of beamline MX14.1 operated by the Helmholtz-Zentrum Berlin at the BESSY II electron storage ring (Berlin-Adlershof, Germany) to collect diffraction data is gratefully acknowledged.

■ ABBREVIATIONS

DLBCL-ABC, Diffuse large B-cell lymphoma, subtype-activated B-cell; DLBCL-GCB, Diffuse large B-cell lymphoma, subtype-germinal center B-cell; MCL, mantle cell lymphoma; BL, Burkitt lymphoma; CML, chronic myelogenous leukemia; ALL, acute lymphoblastic leukemia; AML, acute monocytic leukemia

■ REFERENCES

(1) Rosenthal, A.; Younes, A. High grade B-cell lymphoma with rearrangements of MYC and BCL2 and/or BCL6: Double hit and

triple hit lymphomas and double expressing lymphoma. *Blood Rev.* **2017**, *31*, 37–42.

(2) Choe, H.; Ruan, J. Next Generation of Targeted Molecules for Non-Hodgkin Lymphomas: Small-Molecule Inhibitors of Intracellular Targets and Signaling Pathways. *Oncology* **2016**, *30*, 847–858.

(3) Fakhri, B.; Kahl, B. Current and emerging treatment options for mantle cell lymphoma. *Ther. Adv. Hematol.* **2017**, *8*, 223–234.

(4) Horn, H.; Staiger, A. M.; Ott, G. New targeted therapies for malignant lymphoma based on molecular heterogeneity. *Expert Rev. Hematol.* **2017**, *10*, 39–51.

(5) Malumbres, M. Cyclin-dependent kinases. *Genome Biol.* **2014**, *15*, 122.

(6) Bruyère, C.; Meijer, L. Targeting cyclin-dependent kinases in anti-neoplastic therapy. *Curr. Opin. Cell Biol.* **2013**, *25*, 772–779.

(7) Krystof, V.; Uldrijan, S. Cyclin-dependent kinase inhibitors as anticancer drugs. *Curr. Drug Targets* **2010**, *11*, 291–302.

(8) Whittaker, S. R.; Mallinger, A.; Workman, P.; Clarke, P. A. Inhibitors of cyclin-dependent kinases as cancer therapeutics. *Pharmacol. Ther.* **2017**, *173*, 83–105.

(9) Cai, D.; Latham, V. M., Jr.; Zhang, X.; Shapiro, G. I. Combined depletion of cell cycle and transcriptional cyclin-dependent kinase activities induces apoptosis in cancer cells. *Cancer Res.* **2006**, *66*, 9270–9280.

(10) Gelbert, L. M.; Cai, S.; Lin, X.; Sanchez-Martinez, C.; del Prado, M.; Lallena, M. J.; Torres, R.; Ajamie, R. T.; Wishart, G. N.; Flack, R. S.; Neubauer, B. L.; Young, J.; Chan, E. M.; Iversen, P.; Cronier, D.; Kreklau, E.; de Dios, A. Preclinical characterization of the CDK4/6 inhibitor LY2835219: in-vivo cell cycle-dependent/independent anti-tumor activities alone/in combination with gemcitabine. *Invest. New Drugs* **2014**, *32*, 825–837.

(11) Gregory, G. P.; Hogg, S. J.; Kats, L. M.; Vidacs, E.; Baker, A. J.; Gilan, O.; Lefebvre, M.; Martin, B. P.; Dawson, M. A.; Johnstone, R. W.; Shortt, J. CDK9 inhibition by dinaciclib potently suppresses Mcl-1 to induce durable apoptotic responses in aggressive MYC-driven B-cell lymphoma in vivo. *Leukemia* **2015**, *29*, 1437–1441.

(12) Lacrima, K.; Valentini, A.; Lambertini, C.; Taborelli, M.; Rinaldi, A.; Zucca, E.; Catapano, C.; Cavalli, F.; Gianella-Borradori, A.; MacCallum, D. E.; Bertoni, F. In vitro activity of cyclin-dependent kinase inhibitor CYC202 (Seliciclib, R-roscovitine) in mantle cell lymphomas. *Ann. Oncol.* **2005**, *16*, 1169–1176.

(13) Leonard, J. P.; LaCasce, A. S.; Smith, M. R.; Noy, A.; Chirieac, L. R.; Rodig, S. J.; Yu, J. Q.; Vallabhajosula, S.; Schoder, H.; English, P.; Neuberger, D. S.; Martin, P.; Millenson, M. M.; Ely, S. A.; Courtney, R.; Shaik, N.; Wilner, K. D.; Randolph, S.; Van den Abbeele, A. D.; Chen-Kiang, S. Y.; Yap, J. T.; Shapiro, G. I. Selective CDK4/6 inhibition with tumor responses by PD0332991 in patients with mantle cell lymphoma. *Blood* **2012**, *119*, 4597–4607.

(14) Marzec, M.; Kasprzycka, M.; Lai, R.; Gladden, A. B.; Wlodarski, P.; Tomczak, E.; Nowell, P.; Deprimo, S. E.; Sadis, S.; Eck, S.; Schuster, S. J.; Diehl, J. A.; Wasik, M. A. Mantle cell lymphoma cells express predominantly cyclin D1a isoform and are highly sensitive to selective inhibition of CDK4 kinase activity. *Blood* **2006**, *108*, 1744–1750.

(15) Narita, T.; Ishida, T.; Ito, A.; Masaki, A.; Kinoshita, S.; Suzuki, S.; Takino, H.; Yoshida, T.; Ri, M.; Kusumoto, S.; Komatsu, H.; Imada, K.; Tanaka, Y.; Takaori-Kondo, A.; Inagaki, H.; Scholz, A.; Lienau, P.; Kuroda, T.; Ueda, R.; Iida, S. Cyclin-dependent kinase 9 is a novel specific molecular target in adult T-cell leukemia/lymphoma. *Blood* **2017**, *130*, 1114–1124.

(16) Cayrol, F.; Praditsuktavorn, P.; Fernando, T. M.; Kwiatkowski, N.; Marullo, R.; Calvo-Vidal, M. N.; Phillip, J.; Pera, B.; Yang, S. N.; Takpradit, K.; Roman, L.; Gaudiano, M.; Crescenzo, R.; Ruan, J.; Inghirami, G.; Zhang, T.; Cremaschi, G.; Gray, N. S.; Cerchietti, L. THZ1 targeting CDK7 suppresses STAT transcriptional activity and sensitizes T-cell lymphomas to BCL2 inhibitors. *Nat. Commun.* **2017**, *8*, 14290.

(17) Choudhary, G. S.; Tat, T. T.; Misra, S.; Hill, B. T.; Smith, M. R.; Almasan, A.; Mazumder, S. Cyclin E/Cdk2-dependent phosphor-

ylation of Mcl-1 determines its stability and cellular sensitivity to BH3 mimetics. *Oncotarget* **2015**, *6*, 16912–16925.

(18) Dey, J.; Deckwerth, T. L.; Kerwin, W. S.; Casalini, J. R.; Merrell, A. J.; Grenley, M. O.; Burns, C.; Ditzler, S. H.; Dixon, C. P.; Beirne, E.; Gillespie, K. C.; Kleinman, E. F.; Klinghoffer, R. A. Voruciclib, a clinical stage oral CDK9 inhibitor, represses MCL-1 and sensitizes high-risk diffuse large B-cell lymphoma to BCL2 inhibition. *Sci. Rep.* **2017**, *7*, 18007.

(19) Li, L.; Pongtornpipat, P.; Tiutan, T.; Kendrick, S. L.; Park, S.; Persky, D. O.; Rimsza, L. M.; Puvvada, S. D.; Schatz, J. H. Synergistic induction of apoptosis in high-risk DLBCL by BCL2 inhibition with ABT-199 combined with pharmacologic loss of MCL1. *Leukemia* **2015**, *29*, 1702–1712.

(20) Phillips, D. C.; Xiao, Y.; Lam, L. T.; Litvinovich, E.; Roberts-Rapp, L.; Souers, A. J.; Levenson, J. D. Loss in MCL-1 function sensitizes non-Hodgkin's lymphoma cell lines to the BCL-2-selective inhibitor venetoclax (ABT-199). *Blood Canc. J.* **2015**, *5*, No. e368.

(21) Yecies, D.; Carlson, N. E.; Deng, J.; Letai, A. Acquired resistance to ABT-737 in lymphoma cells that up-regulate MCL-1 and BFL-1. *Blood* **2010**, *115*, 3304–3313.

(22) Havlíček, L.; Hanus, J.; Veselý, J.; Leclerc, S.; Meijer, L.; Shaw, G.; Strnad, M. Cytokinin-derived cyclin-dependent kinase inhibitors: synthesis and cdc2 inhibitory activity of olomoucine and related compounds. *J. Med. Chem.* **1997**, *40*, 408–412.

(23) Meijer, L.; Raymond, E. Roscovitine and other purines as kinase inhibitors. From starfish oocytes to clinical trials. *Acc. Chem. Res.* **2003**, *36*, 417–425.

(24) Gucký, T.; Jorda, R.; Zatloukal, M.; Bazgier, V.; Berka, K.; Řezníčková, E.; Béres, T.; Strnad, M.; Kryštof, V. A novel series of highly potent 2,6,9-trisubstituted purine cyclin-dependent kinase inhibitors. *J. Med. Chem.* **2013**, *56*, 6234–6247.

(25) Haider, C.; Grubinger, M.; Reznickova, E.; Weiss, T. S.; Rotheneder, H.; Miklos, W.; Berger, W.; Jorda, R.; Zatloukal, M.; Gucky, T.; Strnad, M.; Krystof, V.; Mikulits, W. Novel inhibitors of cyclin-dependent kinases combat hepatocellular carcinoma without inducing chemoresistance. *Mol. Cancer Ther.* **2013**, *12*, 1947–1957.

(26) Zatloukal, M.; Jorda, R.; Gucký, T.; Řezníčková, E.; Voller, J.; Pospíšil, T.; Malínková, V.; Adamcová, H.; Kryštof, V.; Strnad, M. Synthesis and in vitro biological evaluation of 2,6,9-trisubstituted purines targeting multiple cyclin-dependent kinases. *Eur. J. Med. Chem.* **2013**, *61*, 61–72.

(27) El Hage, K.; Piquemal, J.-P.; Oumata, N.; Meijer, L.; Galons, H.; Gresh, N. A simple somerization of the purine scaffold of a kinase inhibitor, roscovitine, affords a four- to seven-fold enhancement of its affinity for four CDKs. Could this be traced back to conjugation-induced stiffenings/loosenings of rotational barriers? *ACS Omega* **2017**, *2*, 3467–3474.

(28) Jorda, R.; Havlíček, L.; McNae, I. W.; Walkinshaw, M. D.; Voller, J.; Sturc, A.; Navrátilová, J.; Kuzma, M.; Mistrík, M.; Bártek, J.; Strnad, M.; Kryštof, V. Pyrazolo[4,3-d]pyrimidine bioisostere of roscovitine: evaluation of a novel selective inhibitor of cyclin-dependent kinases with antiproliferative activity. *J. Med. Chem.* **2011**, *54*, 2980–2993.

(29) Řezníčková, E.; Weitensteiner, S.; Havlíček, L.; Jorda, R.; Gucký, T.; Berka, K.; Bazgier, V.; Zahler, S.; Kryštof, V.; Strnad, M. Characterization of a pyrazolo[4,3-d]pyrimidine inhibitor of cyclin-dependent kinases 2 and 5 and aurora A with pro-apoptotic and anti-angiogenic activity in vitro. *Chem. Biol. Drug Des.* **2015**, *86*, 1528–1540.

(30) Vymětalová, L.; Havlíček, L.; Šturc, A.; Skrášková, Z.; Jorda, R.; Pospíšil, T.; Strnad, M.; Kryštof, V. 5-Substituted 3-isopropyl-7-[4-(2-pyridyl)benzyl]amino-1(2H)-pyrazolo[4,3-d]pyrimidines with anti-proliferative activity as potent and selective inhibitors of cyclin-dependent kinases. *Eur. J. Med. Chem.* **2016**, *110*, 291–301.

(31) Havlíček, L.; Moravcová, D.; Kryštof, V.; Strnad, M. The identification of a novel highly condensed pentacyclic heteroaromatic ring system 1,3,5,5b,6,8,10,10b-octaazacyclopenta[h,i]aceanthrylene and its application in the synthesis of 5,7-substituted pyrazolo[4,3-d]pyrimidines. *J. Heterocycl. Chem.* **2015**, *52*, 669–673.

(32) Molinsky, J.; Klanova, M.; Koc, M.; Beranova, L.; Andera, L.; Ludvikova, Z.; Bohmova, M.; Gasova, Z.; Strnad, M.; Ivanek, R.; Trneny, M.; Necas, E.; Zivny, J.; Klener, P. Roscovitine sensitizes leukemia and lymphoma cells to tumor necrosis factor-related apoptosis-inducing ligand-induced apoptosis. *Leuk. Lymphoma* **2013**, *54*, 372–380.

(33) Nekardová, M.; Vymětalová, L.; Khirsariya, P.; Kováčová, S.; Hylsová, M.; Jorda, R.; Kryštof, V.; Fanfrlík, J.; Hobza, P.; Paruch, K. Structural basis of the interaction of cyclin-dependent kinase 2 with roscovitine and its analogues having bioisosteric central heterocycles. *ChemPhysChem* **2017**, *18*, 785–795.

(34) Chang, Y.-T.; Gray, N. S.; Rosania, G. R.; Sutherlin, D. P.; Kwon, S.; Norman, T. C.; Sarohia, R.; Leost, M.; Meijer, L.; Schultz, P. G. Synthesis and application of functionally diverse 2,6,9-trisubstituted purine libraries as CDK inhibitors. *Chem. Biol.* **1999**, *6*, 361–375.

(35) Demange, L.; Abdellah, F. N.; Lozach, O.; Ferandin, Y.; Gresh, N.; Meijer, L.; Galons, H. Potent inhibitors of CDK5 derived from roscovitine: synthesis, biological evaluation and molecular modelling. *Bioorg. Med. Chem. Lett.* **2013**, *23*, 125–131.

(36) N'gompaza-Diarra, J.; Bettayeb, K.; Gresh, N.; Meijer, L.; Oumata, N. Synthesis and biological evaluation of selective and potent cyclin-dependent kinase inhibitors. *Eur. J. Med. Chem.* **2012**, *56*, 210–216.

(37) Wilson, S. C.; Atrash, B.; Barlow, C.; Eccles, S.; Fischer, P. M.; Hayes, A.; Kelland, L.; Jackson, W.; Jarman, M.; Mirza, A.; Moreno, J.; Nutley, B. P.; Raynaud, F. I.; Sheldrake, P.; Walton, M.; Westwood, R.; Whittaker, S.; Workman, P.; McDonald, E. Design, synthesis and biological evaluation of 6-pyridylmethylaminopurines as CDK inhibitors. *Bioorg. Med. Chem.* **2011**, *19*, 6949–6965.

(38) Paruch, K.; Dwyer, M. P.; Alvarez, C.; Brown, C.; Chan, T.-Y.; Doll, R. J.; Keertikar, K.; Knutson, C.; McKittrick, B.; Rivera, J.; Rossmann, R.; Tucker, G.; Fischmann, T. O.; Hruza, A.; Madison, V.; Nomeir, A. A.; Wang, Y.; Lees, E.; Parry, D.; Sgambellone, N.; Seghezzi, W.; Schultz, L.; Shanahan, F.; Wiswell, D.; Xu, X.; Zhou, Q.; James, R. A.; Paradkar, V. M.; Park, H.; Rokosz, L. R.; Stauffer, T. M.; Guzi, T. J. Pyrazolo[1,5-a]pyrimidines as orally available inhibitors of cyclin-dependent kinase 2. *Bioorg. Med. Chem. Lett.* **2007**, *17*, 6220–6223.

(39) Bettayeb, K.; Oumata, N.; Echalié, A.; Ferandin, Y.; Endicott, J. A.; Galons, H.; Meijer, L. CR8, a potent and selective, roscovitine-derived inhibitor of cyclin-dependent kinases. *Oncogene* **2008**, *27*, 5797–5807.

(40) Oumata, N.; Bettayeb, K.; Ferandin, Y.; Demange, L.; Lopez-Giral, A.; Goddard, M.-L.; Myrianthopoulos, V.; Mikros, E.; Flajolet, M.; Greengard, P.; Meijer, L.; Galons, H. Roscovitine-derived, dual-specificity inhibitors of cyclin-dependent kinases and casein kinases I. *J. Med. Chem.* **2008**, *51*, 5229–5242.

(41) Sroka, I. M.; Heiss, E. H.; Havlíček, L.; Totzke, F.; Aristei, Y.; Pechan, P.; Kubbutat, M. H. G.; Strnad, M.; Dirsch, V. M. A novel roscovitine derivative potently induces G1-phase arrest in platelet-derived growth factor-BB-activated vascular smooth muscle cells. *Mol. Pharmacol.* **2010**, *77*, 255–261.

(42) Klanova, M.; Andera, L.; Brazina, J.; Svadlenka, J.; Benesova, S.; Soukup, J.; Prukova, D.; Vejmelkova, D.; Jaksá, R.; Helman, K.; Vockova, P.; Lateckova, L.; Molinsky, J.; Maswabi, B. C. L.; Alam, M.; Kodet, R.; Pytlík, R.; Trneny, M.; Klener, P. Targeting of BCL2 family proteins with ABT-199 and homoharringtonine reveals BCL2- and MCL1-dependent subgroups of diffuse large B-cell lymphoma. *Clin. Cancer Res.* **2016**, *22*, 1138–1149.

(43) Wenzel, S.-S.; Grau, M.; Mavis, C.; Hailfinger, S.; Wolf, A.; Madle, H.; Deeb, G.; Dörken, B.; Thome, M.; Lenz, P.; Dirmhofer, S.; Hernandez-Ilizaliturri, F. J.; Tzankov, A.; Lenz, G. MCL1 is deregulated in subgroups of diffuse large B-cell lymphoma. *Leukemia* **2013**, *27*, 1381–1390.

(44) Mesropyan, E. G.; Galstyan, A. S.; Avetisyan, A. A. Syntheses on the basis of 4-(oxiran-2-ylmethyl)morpholine. *Russ. J. Org. Chem.* **2006**, *42*, 1845–1847.

(45) Fontana, E.; Giribone, D.; Felicini, C. Synthesis of PHA-690509 labelled with ^{14}C . *J. Labelled Compd. Radiopharm.* **2007**, *50*, 225–227.

(46) Watson, I. D. G.; Afagh, N.; Yudin, A. K. Cyclohexene Imine. *Org. Synth.* **2010**, *87*, 161–169.

(47) Perrault, W. R.; Pearlman, B. A.; Godrej, D. B.; Jeganathan, A.; Yamagata, K.; Chen, J. J.; Lu, C. V.; Herrinton, P. M.; Gadwood, R. C.; Chan, L.; Lyster, M. A.; Maloney, M. T.; Moeslein, J. A.; Greene, M. L.; Barbachyn, M. R. The Synthesis of N-Aryl-5(S)-aminomethyl-2-oxazolidinone Antibacterials and Derivatives in One Step from Aryl Carbamates. *Org. Process Res. Dev.* **2003**, *7*, 533–546.

(48) Campbell, K. N.; Sommers, A. H.; Campbell, B. K. tert-Butylamine [I. Hydrogenolysis of 2,2-dimethylethylenimine]. *Org. Synth.* **1947**, *27*, 12.

(49) Engler, A. C.; Bonner, D. K.; Buss, H. G.; Cheung, E. Y.; Hammond, P. T. The synthetic tuning of clickable pH responsive cationic polypeptides and block copolypeptides. *Soft Matter* **2011**, *7*, 5627–5637.

(50) Jorda, R.; Hendrychová, D.; Voller, J.; Řezníčková, E.; Gucký, T.; Kryštof, V. How selective are pharmacological inhibitors of cell-cycle-regulating cyclin-dependent kinases? *J. Med. Chem.* **2018**, *61*, 9105–9120.

(51) Mueller, U.; Darowski, N.; Fuchs, M. R.; Förster, R.; Hellmig, M.; Paithankar, K. S.; Pühringer, S.; Steffien, M.; Zocher, G.; Weiss, M. S. Facilities for macromolecular crystallography at the Helmholtz-Zentrum Berlin. *J. Synchrotron Radiat.* **2012**, *19*, 442–449.

(52) Kabsch, W. XDS. *Acta Crystallogr., Sect. D: Biol. Crystallogr.* **2010**, *66*, 125–132.

(53) XDSGUI. <https://sbgrid.org/software/titles/xdsgui> (accessed 3 March, 2018).

(54) Vagin, A.; Teplyakov, A. MOLREP: an automated program for molecular replacement. *J. Appl. Crystallogr.* **1997**, *30*, 1022–1025.

(55) Hylšová, M.; Carbain, B.; Fanfrlík, J.; Musilová, L.; Haldar, S.; Köprülüoğlu, C.; Ajani, H.; Brahmshatriya, P. S.; Jorda, R.; Kryštof, V.; Hobza, P.; Echalié, A.; Paruch, K.; Lepšík, M. Explicit treatment of active-site waters enhances quantum mechanical/implicit solvent scoring: Inhibition of CDK2 by new pyrazolo[1,5-*a*]pyrimidines. *Eur. J. Med. Chem.* **2017**, *126*, 1118–1128.

(56) Murshudov, G. N.; Vagin, A. A.; Dodson, E. J. Refinement of macromolecular structures by the maximum-likelihood method. *Acta Crystallogr., Sect. D: Biol. Crystallogr.* **1997**, *53*, 240–255.

(57) Collaborative Computational Project, Number 4. The CCP4 suite: programs for protein crystallography. *Acta Crystallogr., Sect. D: Biol. Crystallogr.* **1994**, *50*, 760–763.

(58) Emsley, P.; Cowtan, K. Coot: model-building tools for molecular graphics. *Acta Crystallogr., Sect. D: Biol. Crystallogr.* **2004**, *60*, 2126–2132.

(59) Chen, V. B.; Arendall, W. B., III; Headd, J. J.; Keedy, D. A.; Immormino, R. M.; Kapral, G. J.; Murray, L. W.; Richardson, J. S.; Richardson, D. C. MolProbity: all-atom structure validation for macromolecular crystallography. *Acta Crystallogr., Sect. D: Biol. Crystallogr.* **2010**, *66*, 12–21.

(60) Schrodinger, LLC. *The PyMOL Molecular Graphics System*, version 1.3r1, 2010.